NUMERICAL ANALYSIS OF CRACKED PLATES IN BENDING

by

LT. S. SANT

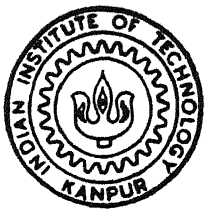

DEPARTMENT OF MECHANICAL ENGINEERING

INDIAN INSTITUTE OF TECHNOLOGY KANPUR

February 1994

NUMERICAL ANALYSIS OF CRACKED PLATES IN BENDING

A Thesis Submitted
In Partial Fulfillment of the Requirements

for the Degree of
MASTER OF TECHNOLOGY

By
LT. S. SANT

to the
DEPARTMENT OF MECHANICAL ENGINEERING
INDIAN INSTITUTE OF TECHNOLOGY
KANPUR

February 1994

CERTIFICATE

7.2

This is to certify that this work entitled "NUMERICAL ANALYSIS OF CRACKED PLATES IN BENDING" by LT. S. Sant has been carried out under my supervision and has not been submitted elsewhere for a degree.

(Dr P.M. Dixit)
Associate Professor
Department of Mechanical Engineering
I.I.T. Kanpur

Feb. 94

ACKNOWLEDGEMENTS

I am extremely grateful to Dr. P.M. Dixit and, express my deep sense of gratitude and indebtedness to him for his valuable guidance, and consistent inspiration throughout the work.

I am extremely thankful to Dr Prashant Kumar, Dr N.N. Kishore and Dr R. Sethuraman for their valuable suggestions and willingness to help at all stages of the work.

I am very grateful to Dr. S.G. Dhande for extending timely help in successful completion of this work.

It was a great pleasure to work with, Raghuraman, Umesh and Ashok. Their company was lively and words are just not enough to express my thanks for the valuable help they extended, at all stages of the work.

Finally I am extremely grateful to the Indian Navy for sending me to do this course.

LT. S. Sant

CONTENTS

ABSTRACT

Presence of cracks in hull plates of submarine/ship is undesirable as it reduces the strength and efficiency of the vessel. Further underwater shocks created by mines torpedo etc. might lead to propagation of these cracks. It is important to know the parameters which lead to propagation of these cracks, resulting in a catastrophic failure. Stress intensity factor (SIF) is the most widely used parameter in static problems.

The problem of submarine hull modelling is complex as it falls under the framework of dynamic elasto-plastic analysis. As a first attempt one can do static, linear elastic analysis to get an insight into the complex nature of the problem. In the present work a part of submarine hull bounded by two stiffening rings is idealised a plate. It is assumed that cracks are either parallel or perpendicular to stiffening rings, and the loading is transverse and uniform. As the submarine hull plate is considerably thick, Mindlin's plate theory has been used in formulating the problem. The problem is solved using the Finite Element technique. Stress intensity factor in mode I has been evaluated using the J integral approach.

Effect of plate length, distance between the edges perpendicular to stiffening rings, crack orientation and the boundary conditions on the edges perpendicular to stiffening rings on the normalised stress intensity factor have been studied. It has been found that SIF increases as the distance between the edges perpendicular to stiffening rings is increased It is also found to increase as the crack orientation changes from parallel to perpendicular, and the boundary conditions change from simply supported to free on edges perpendicular to stiffening rings. It is found that a perpendicular crack with free ends is the most dangerous.

ABSTRACT

Presence of cracks in hull plates of submarine/ship is undesirable as it reduces the strength and efficiency of the vessel. Further underwater shocks created by mines torpedo etc. might lead to propagation of these cracks. It is important to know the parameters which lead to propagation of these cracks, resulting in a catastrophic failure. Stress intensity factor (SIF) is the most widely used parameter in static problems.

The problem of submarine hull modelling is complex as it falls under the framework of dynamic elasto-plastic analysis. As a first attempt one can do static, linear elastic analysis to get an insight into the complex nature of the problem. In the present work a part of submarine hull bounded by two stiffening rings is idealised a plate. It is assumed that cracks are either parallel or perpendicular to stiffening rings, and the loading is transverse and uniform. As the submarine hull plate is considerably thick, Mindlin's plate theory has been used in formulating the problem. The problem is solved using the Finite Element technique. Stress intensity factor in mode I has been evaluated using the J integral approach.

Effect of plate length, distance between the edges perpendicular to stiffening rings, crack orientation and the boundary conditions on the edges perpendicular to stiffening rings on the normalised stress intensity factor have been studied. It has been found that SIF increases as the distance between the edges perpendicular to stiffening rings is increased It is also found to increase as the crack orientation changes from parallel to perpendicular, and the boundary conditions change from simply supported to free on edges perpendicular to stiffening rings. It is found that a perpendicular crack with free ends is the most dangerous.

LIST OF FIGURES

LIST OF SYMBOLS

a	Semi crack length
B	Half plate width
$[B]$	Strain displacement matrix
$[D]_b$	Elasticity matrix (bending)
$[D]_s$	Elasticity matrix (shear)
E	Modulus of elasticity
$\{f_i\}^e$	Body force vector
$\{f_i\}^b$	Surface force vector on specified boundary
$\{F\}$	Global force vector
h	Plate thickness
J_x, J_y	Path independent integrals
$[J]$	Jacobian matrix
$[J]^{-1}$	Inverse of $[J]$
K_1, K_2, K_3	Stress intensity factors in mode I, II and III respectively
$\tilde{K}_1$	Normalised stress intensity factor
$[K]$	Global stiffness matrix
L	Length of plate
$[N]$	Shape functions
P_z	Uniform transverse load
r	Radial distance from crack tip
t	Plate thickness
U	Strain energy density factor
u	Displacement in x direction
v	Displacement in y direction
w	Displacement in z direction
W	Strain energy density

Greek Symbols

(ϵ)	Strains
θ_x	Rotation about y axis
θ_y	Rotation about negative x axis
ν	Poisson ratio
ξ, η, ζ	Natural coordinates
$\{\chi\}$	Curvatures
$\{\sigma\}$	Stresses
ψ_x	Rotation about y axis
ψ_y	Rotation about x axis

CHAPTEAR I

INTRODUCTION

1.1 INTRODUCTION

Submarine hull or pressure hull is basically fabricated by welding of plates which are mounted on circumferential stiffening rings. Presence of cracks in hull plates is undesirable as it reduces the strength and efficiency of the vessel. Cracks can be present as inherent defects in manufactured components or may originate during service due to damages. Cracks may also emanate from stress concentration points due to fatigue or may be present as defects in welded joints during fabrication. The capacity of a plate to withstand external pressure pulse/transverse load reduces due to the presence of cracks. Further high intensity underwater shocks created by mines torpedo etc. lead to propagation of these cracks which might lead to catastrophic failure. As the residual strength is a function of crack size, it is essential to analyse a cracked plate in bending so as to determine the extent to which strength is reduced, and how this is related to crack size. The analysis also helps in determining maximum size of crack that can be tolerated and, time required for the crack to grow to critical size.

A hull plate mounted on two adjacent stiffening rings can be localised for analysis/study of crack propagation in submarine hull due to underwater explosion. As the pressure pulse created

by underwater explosion acts for a short duration of time and as the submarine hull behaves like an elasto plastic material at high stress level, the problem falls under the frame-work of dynamic elasto-plastic analysis. A dynamic problem with elasto plastic mataerial behaviour will correctly model the problem and will give accurate results for fracture parameters, but it is difficult to analyse such problem. A rough estimate of fracture parameters can be obtained by analysing the problem within the framework of static elastic analysis. Although the values obtained may be approximate, the trend of variation of fracture parameters with respect to geometric variables such as crack length, plate thickness, aspect ratio of plate etc., is similar to the one predicted by dynamic elasto-plastic analysis. Thus static elastic analysis gives an insight into the complex nature of the problem and forms a base for dynamic elasto plastic analysis.

1.2 LITERATURE SURVEY

Stresses in the region near the crack tip are large and their distribution is complex. Several investigators have discussed the nature of the local stresses around a sharp crack in plates subjected to transverse loading. Williams [1] found that elastic bending stresses near the tip of a semi-infinite crack vary as the inverse square-root of the radial distance from the crack front. The magnitude of the stresses was left undetermined in his analysis. It was Sih and Rice [2,3] who later determined this magnitude by using the theory of complex functions. The results in [1-3] were obtained from the classical fourth order Kirchoff theory of thin plates, which has two short comings. The first one

is that the edge conditions at the crack surface are satisfied only in an approximate manner in that the three physically natural boundary conditions of prescribing bending moment, twisting moment and transverse shear are replaced by two conditions. Owing to such a replacement, the stress distribution in the immediate neighbourhood of the crack edges will naturally be affected and will not be accurate. The second limitation of Kirchoff theory is that transverse shear effects are neglected. Near a crack tip in a plate, the gradients of the in-plane stress components are very large. This induces a large variation of the transverse displacement in the plane-of the plate. This means an extremely large transverse shear strain and the associated transverse shear stresses.

The theories which include the effect of transverse shear deformation and which make it possible to satisfy all the boundary conditions along a stress free edge are due Mindlin [4] and Reissner [5]. Knowles and Wang [6] applied the Reissner theory making use of the integral transform technique, to obtain an approximate solution for the crack tip stresses in a plate with vanishingly small thickness. It was found that the order of the singularity of the boundary stresses near a crack tip was the same as classical theory [1] but the angular distributions were not dependent on Poisson's ratio like in the classical theory. Hartrancraft and Sih [7] applied the Reissner theory using another method of solution to study the effect of plate thickness on the bending stresses in the vicinity of the crack-front. He showed that, unlike in classical plate theory, the stress intensity

factor (SIF) depends strongly on the plate thickness. For a typical problem, the SIF was found to vary very rapidly in the range of $0 < h/a < 0.25$ where h is the plate thickness and a is the half crack length.

The above solutions based on the Reissner theory establish only the functional form of singular stresses and not the general crack tip solution of William's type [1]. Such a general solution was first provided by Murthy et al [8]. The solution includes complete class of solutions expressed in terms of polar coordinates at the crack tip. It was observed that standard numerical techniques like collocation, successive integration etc. fail to give satisfactory convergence for SIF in plates with large plate sizes ($l/a > 1$), and small thickness ratio ($h/a < 0.5$). It was shown that such limitations in numerical analysis arose mainly due to the mathematical nature of continuum solution which involves Bessel functions with large arguments. This is a severe limitation because the parameters l/a and h/a, in practice, do fall in the ranges mentioned.

Although continuum solutions do give accurate picture of the singular stresses, their applicability is confined mostly to infinite domains. For general applicability, the finite element method (FEM) appears to be a logical choice because of its elegance, flexibility and applicability to large classes of geometries, materials and loading conditions. The various finite element formulations, with special reference to plate bending problem, have been reviewed by Wahaba [9]. Following three approaches are usually followed in treating the singularity while

formulating special displacement methods.

In the first method, general crack-tip solutions from a continuum solution are chosen as the displacement field for the crack tip element. For convenience (SIF) is chosen as a degree of freedom. However, very few such formulations are available for plate bending case. Most of them are based on classical thin plate theory and thus do not account for the effect of plate thickness. However, the special crack tip element developed by Viswanath et al [10] is based on the sixth order plate theory. As a result it satisfies all the three natural conditions on the crack surface and accounts for the transverse shear deformation. The element can be of any arbitrary shape. A special feature of the element formulation is that only line integrations are involved in setting up of element stiffness matrix. Numerical studies reveal that there exists, an optimum crack tip element size for the given plate thickness which gives the best possible value of the stress intensity factor. The other limitation of this method is that nodal displacements become rather inaccurate at an infinitesimal distance from the crack. This limitation however can be overcome by refining the Mesh near the crack tip.

In the second method, only the term corresponding to singular component of stress is considered from the analytical solution and is superposed on regular polynomials for the displacements in element development. Yagwa and Nishioka [11] have used this method to develop an 8-noded isoparametric element for plate bending. Although the effect of transverse shear deformation is included in the element, the normal displacement at the crack tip

is still based on the Kirchoff assumption.

In the third alternative, singularity is achieved through the Jacobian determinant of the isoparametric element vanishing at the crack tip. A number of special crack tip elements have been developed from the standard isoparametric element enabling the singularity of the strain field at the crack tip to be modelled. Yamada [12] has summarised the development of singularity elements and has elucidated the correlations between proposals which take seemingly different forms. He has also shown that significant improvement is achieved in the estimate of stress intensity factor by the use of singular elements. Barosum [13,14] has developed the quarter point quadratic singular element achieving the inverse square root singularity characteristic. The singularity is achieved by placing the mid side nodes near the crack tip at quarter points. The element contains the necessary rigid body modes and constant strain modes. Further, the element satisfies the continuity requirements of the displacements as well as rotations. The element is applicable to thick as well as thin plates. Since the shear deformation is included and it is possible to satisfy all the three natural boundary conditions, accuracy of the element is very high when compared with other results [7] obtained using Reissner theory. This is in spite of the fact that the element does not have the exact trigonometric angular distribution of stresses around the crack. It is found that four or more elements are sufficient to achieve this variation. Barosum [13,14] determined that by collapsing one side of a quadrilateral to form a triangular element in two dimensional

problems and one face of a brick to form a prismatic element in three dimensional problems, far better results are obtained. Barosum also showed that triangular elements possess the same singularity in all directions.

In addition they can have either $1/\sqrt{r}$ singularity representing perfectly elastic behaviour, or $1/r$ singularity representing perfectly plastic behaviour. These are achieved by having either one-node or multiple independent nodes at crack tip respectively. The ease of using these elements, as they exist in many general purpose programs, as well as their high accuracy makes them very attractive for application in linear fracture mechanics problems of plate and shell bending.

There are various parameters called as fracture parameters, which can predict the initiation and propagation of cracks. If these parameters for a given problem can be determined analytically, numerically or experimentally and if critical values of these parameters for the given material are known from experiments, premature failures can be avoided. Most of the above references consider stress intensity factor (K) as the fracture parameter. Linear elastic fracture mechanics is based on the premise that the intensity of stress or strain field surrounding a crack tip may be uniquely described in terms of K. Thus, K can be viewed as a parameter characterising the resistance of metals to both static and fatigue fracture. The physical significance of the stress intensity factor approach is that it can be used as a design parameter to determine the nature of fracture process or used to determine the residual life of a component subjected to

dynamic loading. Besides depending on the applied loading, geometry of the plate, crack size and location it also depends on the mode of fracture. There are three basic modes associated with Plate Bending problems. They are

Mode I : bending mode

Mode II : twisting mode

Mode III : shear mode

First two modes are characterised by moment intensity factor while shear mode is represented by shear force intensity factor. The bulk of fracture mechanics work has been devoted to mode I analysis. This is due partly to the simplicity of its application and partly to its severity on the component. Cracks which start in single mode may in fact become mixed mode later on during their useful life. Since the concept of K is based on linear elasticity it has limitation both on accuracy and interpretation when materials capable of plastic deformation are considered. This limitation can be overcome by the J integral approach which is discussed in next paragraph.

If the crack tip stresses are not modelled accurately, evaluation of K becomes inaccurate. The fracture parameter which avoids evaluation of crack tip stresses is the vector of J integral. Sosa and Eischen [15] and Sosa and Hermann [16] have proposed path independent integrals J_x and J_y for cracked plates subjected to bending loads using Reissner and Mindlin plate theories. When the strain energies of bending and shear are separated all the three stress intensity factors can be calculated

from the integrals J_x and J_y. This approach makes analysis of mixed mode problems simpler. The most outstanding feature of the J integrals approach is its path independency. This allows calculation of linear, non linear elastic energy release rate and elasto-plastic work remote from the crack tip. This concept can be extended to non-linearly elastic or elasto plastic materials.

In case where linear elastic fracture mechanics is applicable the fracture behaviour can be determined by using strain energy density criterion. Sih [17,18] has proposed that failure occurs when stationary value of the strain energy density factor U reaches some critical value which is determined experimentally. On physical grounds, material elements are capable of storing energy by experiencing volume change (dilatation) and shape change (distortion). Excessive dilatation may result in brittle fracture while excessive distortion may tend to yield the material. The proportion of energy absorbed in dilatation and distortion can be determined for various material properties at locations of the stationary values of strain energy density factor. The direction of crack initiation as predicted from the strain energy density theory depends on the intensity of 1/r energy field near the crack tip.

1.3 Objective and Scope

The domain considered is part of the hull bounded by stiffening rings. The limiting dimension in the other direction will be determined from parametric studies. As the thickness to radius ratio is small the domain can be idealised as a plate.

The edges mounted on stiffening rings are considered as fixed

and the distance between these edges is assumed to be constant. The conditions on other two ends do not fall in standard categories. Therefore they are parametrically taken as free and simply supported.

The formulation has been done within the frame work of linear elastic fracture mechanics. The analysis is limited to static loading only. As the thickness of the plate is not small, Mindlin's plate theory has been used to formulate the problem as it accounts for transverse shear deformation effect. Weld joints for securing plates on the stiffening rings are either parallel or perpendicular to rings. As cracks originate from weld joints it is assumed that cracks are either parallel or perpendicular to rings.

Finite element method (FEM) has been used to solve the problem. Collapsed quarter point elements have been used to model the crack tip while quadrilateral isoparametric elements are used in the rest of the domain. In the present study, J integral approach has been used to evaluate the stress intensity factor (K). Because of symmetry of geometry, boundary conditions and loading, K_2 and K_3 are very small, and as such only K_1 has been evaluated. Parametric study has been done to investigate the effects of crack length, plate length, plate thickness and crack orientation on SIF.

1.4 Plan of Thesis

After the introduction, Chapter II presents finite element modelling and formulation of the problem. Chapter III includes test problems, results of parametric study and conclusion.

CHAPTER II

FINITE ELEMENT FORMULATION

In this chapter finite element formulation of a cracked plate subjected to transverse load, using Mindlin's plate theory is presented. It has been assumed while formulating the problem that the material is isotropic, stress strain relationship is linear and the deformation is small within the zone of loading. Singular elements have been used at the crack tip while eight noded isoparametric elements model the rest of domain. J integral approach is used to evaluate the stress intensity factor.

2.1 Mindlin's Plate Theory

The main assumptions of mindlin plate theory are:

(a) Stress component along the normal to the midplane of the plate is negligible.

(b) Transverse displacement does not vary in the thickness direction.

(c) In plane displacements of the midplane are negligible (no membrane effect).

(d) The normal to the midplane remains straight but not necessarily normal to it after deformation.

In classical Kirchoff thin plate theory it is assumed that the normal to the midplane remains normal to it even after deformation. This means that the cross sections do not deform (no

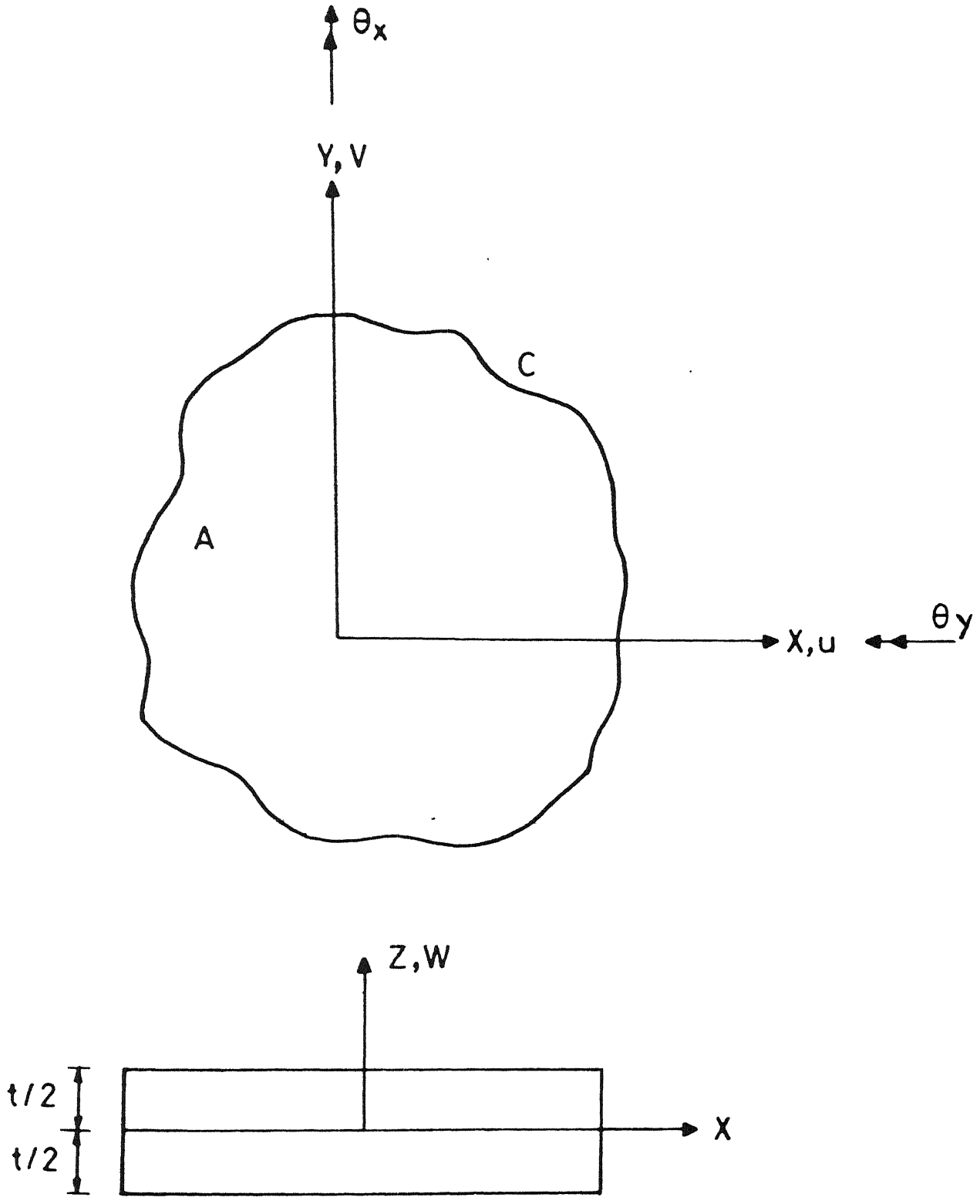

Fig. 2-1

transverse shear deformation) but just rotate relative to each other. However the assumptions of Mindlin plate theory take into account the deformation of cross-section.

The second, third and fourth assumptions lead to the following displacement field

$$\begin{aligned} u &= z\,\theta_x(x,y) \\ v &= z\,\theta_y(x,y) \\ w &= w(x,y) \end{aligned} \tag{2.1}$$

where θ_x and θ_y are counterclockwise rotations about the y and negative x axis respectively as shown in Fig. 2.1.

For small deformation, the strain displacement relations are:

$$\begin{aligned} \epsilon_x &= \frac{\partial u}{\partial x} \\ \epsilon_y &= \frac{\partial v}{\partial y} \\ \epsilon_z &= \frac{\partial w}{\partial x} \\ \gamma_{xy} &= \left(\frac{\partial u}{\partial y} + \frac{\partial v}{\partial x}\right) \\ \gamma_{yz} &= \left(\frac{\partial v}{\partial z} + \frac{\partial w}{\partial y}\right) \\ \gamma_{zx} &= \left(\frac{\partial u}{\partial z} + \frac{\partial w}{\partial x}\right) \end{aligned} \tag{2.2}$$

Substitution of (2.1) in (2.2) gives the strains in terms of θ_x, θ_y and w. Since w is independent of z, $\epsilon_z = 0$. The other strains are

$$\begin{aligned} \epsilon_x &= z\,\frac{\partial \theta_x}{\partial x} \\ \epsilon_y &= z\,\frac{\partial \theta_y}{\partial y} \\ \gamma_{xy} &= z\left(\frac{\partial \theta_x}{\partial y} + \frac{\partial \theta_y}{\partial x}\right) \\ \gamma_{yz} &= \left(\theta_y + \frac{\partial w}{\partial y}\right) \end{aligned} \tag{2.3}$$

$$\gamma_{zx} = \left(\theta_x + \frac{\partial w}{\partial x} \right).$$

The first assumption means $\sigma_z = 0$. Then the stress-strain relations for isotropic linearly elastic material become

$$\sigma_x = \frac{E}{1-\nu^2} (\epsilon_x + \nu \epsilon_y)$$

$$\sigma_y = \frac{E}{1-\nu^2} (\epsilon_y + \nu \epsilon_x)$$

$$\tau_{xy} = \frac{E}{2(1+\nu)} \gamma_{xy} \qquad (2.4)$$

$$\tau_{yz} = \frac{E}{2(1+\nu)} \gamma_{yz}$$

$$\tau_{zx} = \frac{E}{2(1+\nu)} \gamma_{zx}$$

Substitution of (2.3) in (2.4) gives stresses in terms of w, θ_x, θ_y

$$\sigma_x = \frac{Ez}{1-\nu^2} \left(\frac{\partial \theta_x}{\partial x} + \nu \frac{\partial \theta_y}{\partial y} \right)$$

$$\sigma_y = \frac{Ez}{1-\nu^2} \left(\frac{\partial \theta_y}{\partial y} + \nu \frac{\partial \theta_x}{\partial x} \right)$$

$$\tau_{xy} = \frac{Ez}{2(1+\nu)} \left(\frac{\partial \theta_x}{\partial y} + \nu \frac{\partial \theta_y}{\partial x} \right) \qquad (2.5)$$

$$\tau_{yz} = \frac{E}{2(1+\nu)} \left(\theta_y + \frac{\partial w}{\partial y} \right)$$

$$\tau_{zx} = \frac{E}{2(1+\nu)} \left(\theta_x + \frac{\partial w}{\partial x} \right)$$

For a plate bending problem it is more convenient to deal with stress resultants rather than the stresses. The stress resultants are defined as follows :

$$(M_x, M_y, M_{xy}) = \int_{-t/2}^{t/2} z(\sigma_x, \sigma_y, \tau_{xy}) \, dz \qquad (2.6)$$

$$(Q_x, Q_y) = \int_{-t/2}^{t/2} z(\tau_{xz}, \tau_{yz})\, dz \qquad (2.7)$$

where t is the plate thickness. Substitution of (2.5) in (2.6) and (2.7) gives stress resultants in terms of θ_x, θ_y, w.

$$M_x = \frac{Et^3}{12(1-\nu^2)} \left(\frac{\partial \theta_x}{\partial x} + \nu \frac{\partial \theta_y}{\partial y} \right)$$

$$M_y = \frac{Et^3}{12(1-\nu^2)} \left(\frac{\partial \theta_y}{\partial y} + \nu \frac{\partial \theta_x}{\partial x} \right) \qquad (2.8)$$

$$M_{xy} = \frac{Et^3}{24(1+\nu)} \left(\frac{\partial \theta_x}{\partial y} + \nu \frac{\partial \theta_y}{\partial x} \right)$$

$$Q_x = \frac{Et}{2(1+\nu)} \left(\theta_x + \frac{\partial w}{\partial x} \right)$$

$$Q_y = \frac{Et}{2(1+\nu)} \left(\theta_y + \frac{\partial w}{\partial y} \right) \qquad (2.9)$$

According to eqn. (2.5), the shear stresses τ_{yz} and τ_{zx} are constant over the thickness. To take care of variation of τ_{yz} and τ_{zx} the expressions for Q_y and Q_x are multiplied by a factor called as shear correction factor. Eqn. (2.9) then becomes

$$Q_x = \frac{Et\alpha_s}{2(1+\nu)} \left(\theta_x + \frac{\partial w}{\partial x} \right)$$

$$Q_y = \frac{Et\,\alpha_s}{2(1+\nu)} \left(\theta_y + \frac{\partial w}{\partial y} \right) \qquad (2.10)$$

where α_s is the shear correction factor. For subsequent finite element formulation it is convenient to express equations (2.8) and (2.10) in matrix form as follows :

$$\begin{Bmatrix} M_x \\ M_y \\ M_{xy} \end{Bmatrix} = \frac{Et^3}{12(1-\nu^2)} \begin{bmatrix} 1 & \nu & 0 \\ \nu & 1 & 0 \\ 0 & 0 & \frac{(1-\nu)}{2} \end{bmatrix} \begin{Bmatrix} \frac{\partial \theta_x}{\partial x} \\ \frac{\partial \theta_y}{\partial y} \\ \frac{\partial \theta_x}{\partial y} + \frac{\partial \theta_y}{\partial x} \end{Bmatrix} \qquad (2.11)$$

or

$$\{M\} = \{D\}_b \{\chi\}$$

and

$$\begin{Bmatrix} Q_x \\ Q_y \end{Bmatrix} = \frac{\alpha_s Et}{2(1+\nu)} \begin{bmatrix} 1 & 0 \\ 0 & 1 \end{bmatrix} \begin{Bmatrix} \theta_x + \frac{\partial w}{\partial y} \\ \theta_x + \frac{\partial w}{\partial x} \end{Bmatrix} \qquad (2.12)$$

or

$$\{Q\} = \{D\}_s \{\epsilon\}_s$$

where

$\{M\}$ = moment vector

$\{D\}_b$ = Elasticity matrix (bending)

$\{\chi\}$ = curvature vector

$\{Q\}$ = shear force vector

$\{D\}_s$ = Elasticity matrix (shear)

$\{\epsilon\}_s$ = Shear strain vector

The equilibrium equations for a mindlin plate may be written as:

$$\frac{\partial Q_x}{\partial x} + \frac{\partial Q_y}{\partial y} + P_z = 0$$

$$\frac{\partial M_x}{\partial x} + \frac{\partial M_{xy}}{\partial y} - Q_x + \tilde{m}_x = 0 \qquad (2.13)$$

$$\frac{\partial M_{xy}}{\partial x} + \frac{\partial M_y}{\partial y} - Q_y + \tilde{m}_y = 0$$

where P_z = distributed force in z direction

$\tilde{m}_x$ = distributed moment about y axis

$\tilde{m}_y$ = distributed mo ment about negative x-axis.

These equations have to be supplemented by boundary conditions. Typical boundary conditions are discussed in the next paragraph.

The boundary C of the domain (Fig. 2.2) is divided in 3 parts C_1, C_2 and C_3. On C_1, transverse displacement and rotations are specified as :

$$w = w^*, \ \theta_x = \theta_x^* , \ \theta_y = \theta_y^* \tag{2.14}$$

on C_2 shear force and two moment components are specified

$$q = q^*, \ m_x = m_x^*, \ m_y = m_y^* \tag{2.15}$$

where

$$q = Q_x \, n_x + Q_y \, n_y \tag{2.16}$$

$$\begin{Bmatrix} m_x \\ m_y \end{Bmatrix} = \begin{bmatrix} M_x & M_{xy} \\ M_{xy} & M_y \end{bmatrix} \begin{Bmatrix} n_x \\ n_y \end{Bmatrix} \tag{2.17}$$

on C_3, the specified boundary conditions are mixed :

$$w = w^*, \ \theta_s = \theta_s^*, \ m_n = m_n^* \tag{2.18}$$

where

$$\theta_s = \theta_x \, S_x + \theta_y \, S_y \qquad \text{(twist)} \tag{2.19}$$

$$m_n = m_x \ n_x + m_y \, n_y \qquad \text{(bending moment)}$$

In general the problem consisting of differential equations (2.13) and boundary conditions (2.14), (2.15) and (2.18) is difficult to solve analytically. The problem can be solved using the finite element method, for which the total potential energy

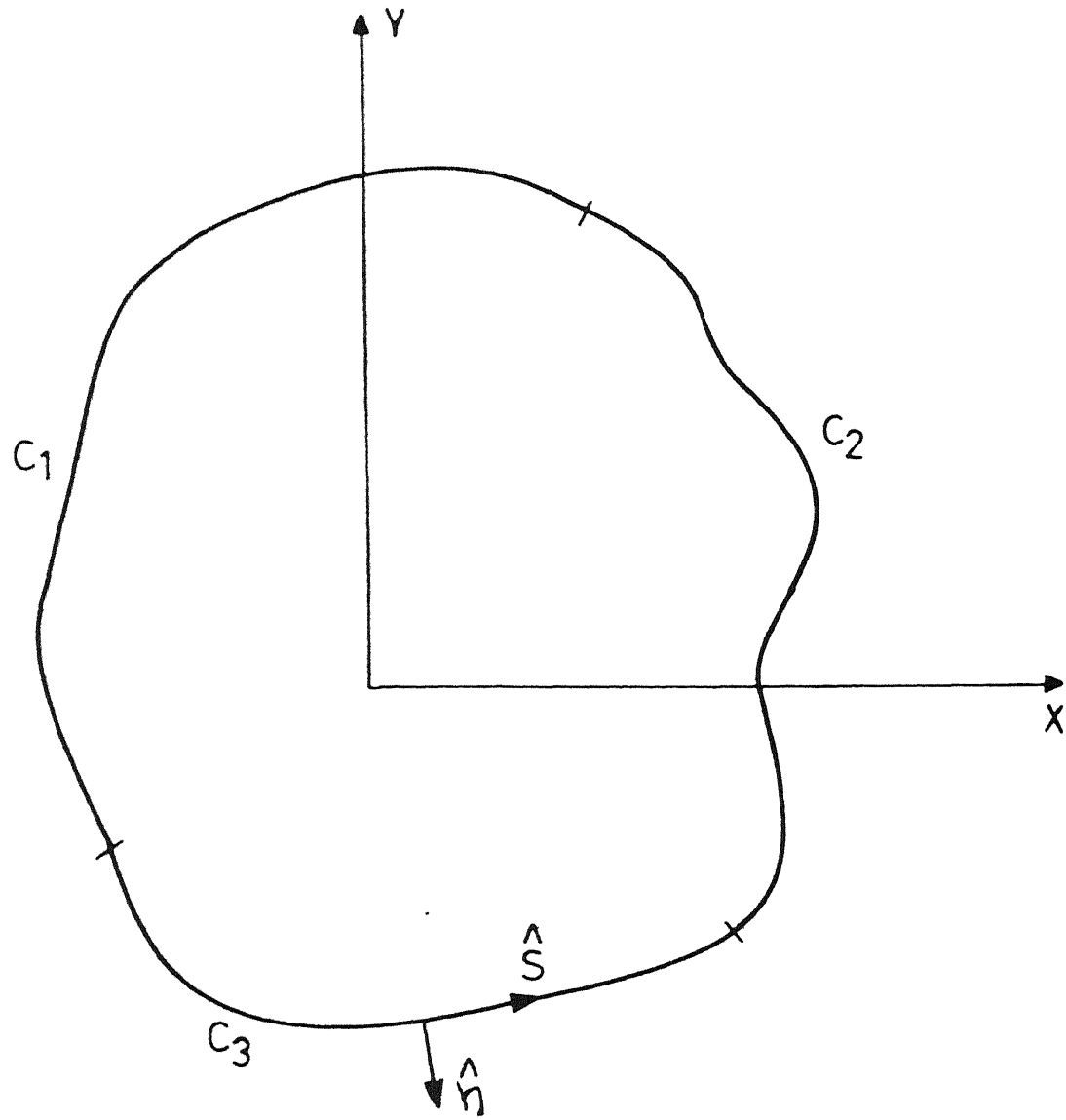

$$\{\hat{n}\} = \begin{Bmatrix} n_x \\ n_y \end{Bmatrix} \qquad \{\hat{S}\} = \begin{Bmatrix} S_x \\ S_y \end{Bmatrix}$$

Fig. 2-2

can be expressed in variational form as :

$$\pi = \frac{1}{2}\int_A \left(\{\chi\}^T [D]_b \{\chi\} + \{\epsilon\}_s^T [D]_s \{\epsilon\}_s \right) dA$$

$$- \int_A \{u\}^T \{b\} dA - \int_{C_2} \{y\}^T \{t\} ds - \int_{C_3} m_n^* \theta_n \, ds \qquad (2.20)$$

where $\{b\}$ = body force vector $\begin{Bmatrix} P_z \\ \tilde{m}_x \\ \tilde{m}_y \end{Bmatrix}$

$\{t\}$ = surface force vector $\begin{Bmatrix} q \\ m_x \\ m_y \end{Bmatrix}$

$\{u\}$ = displacement/rotation vector $\begin{Bmatrix} w \\ \theta_x \\ \theta_y \end{Bmatrix}$.

2.2 Finite Element Formulation

The Finite element method is the most widely used technique which finds an approximate solution by minimising the functional associated with given problem. For the present problem, the functional is the total potential energy given by equation (2.20). The method consists of dividing the domain into a finite number of elements assuming suitable interpolations for the unknown variables over each element and finding the unknown constants in interpolating functions by minimising the functional.

2.2.1 Deriving finite element equations

Finite element formulation based on Mindlin's theory has one important advantage over the one based on classical thin plate theory. Mindlin plate elements require only C^0 continuity of the

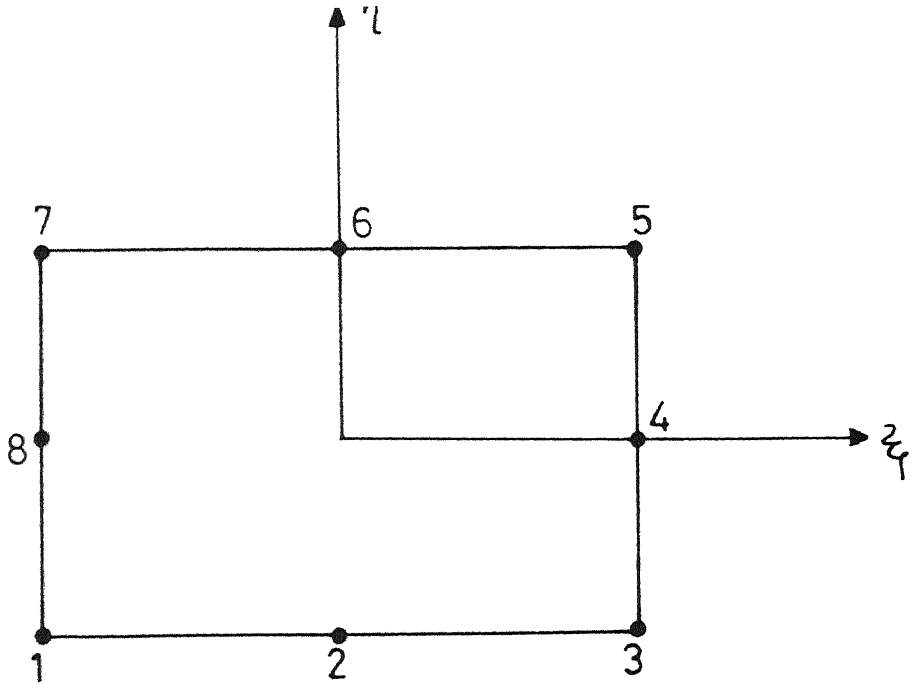

(a)

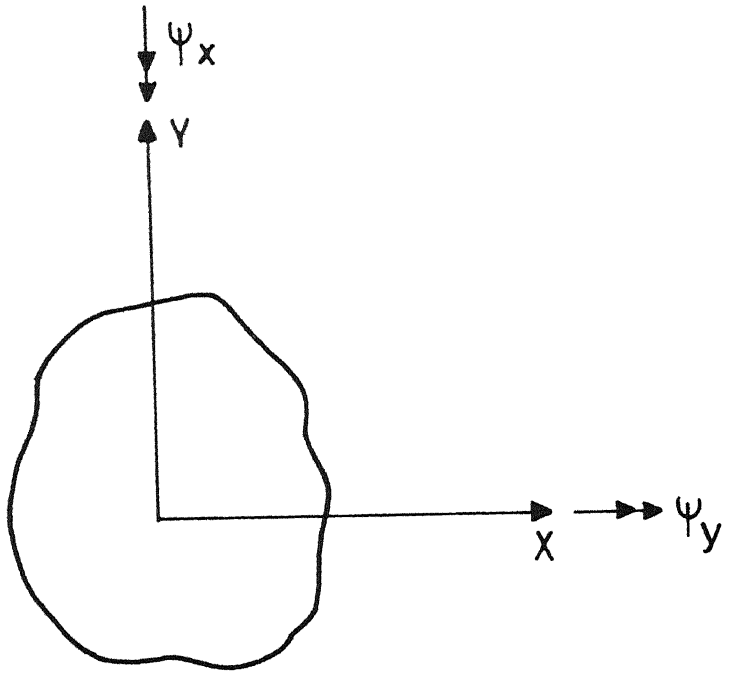

(b)

Fig. 2·3

lateral displacement w and the independent normal rotations θ_x and θ_y. On the other hand elements based on classical Kirchoff thin plate theory need C^1 continuity of w. Thus Mindlin plate elements are simpler to formulate. In the present formulation 8-noded isoparametric elements are used (Fig. 2.3a). Compared to 9 noded Lagrangian elements, these elements are better as they avoid phenomenon of locking in the thin plates.

The displacement and normal rotations at any point in a 8-noded isoparametric element $n^{(e)}$ are give by

$$\begin{Bmatrix} w \\ \theta_x \\ \theta_y \end{Bmatrix} = \sum_{i=1}^{8} \begin{bmatrix} N_i^e & 0 & 0 \\ 0 & -N_i^e & 0 \\ 0 & 0 & -N_i^e \end{bmatrix} \begin{Bmatrix} w_i^e \\ \psi_{xi}^e \\ \psi_{yi}^e \end{Bmatrix} \qquad (2.21)$$

or

$$\{u\} = \sum_{i=1}^{8} [N_i]^e \{a_i\}^e$$

where N_i^e are called shape functions, are known functions expressed in terms of the local coordinates (ξ, η) and the displacement vector $\{a_i\}^e$ contains unknown nodal values of w, θ_x, θ_y. For the sake of convenience rotations have been modified as shown in Fig. 2.3(b). Mathematically

$$\begin{Bmatrix} \theta_x \\ \theta_y \end{Bmatrix} = \begin{bmatrix} -1 & 0 \\ 0 & -1 \end{bmatrix} \begin{Bmatrix} \psi_x \\ \psi_y \end{Bmatrix} \qquad (2.22)$$

when a domain is divided into finite number of elements, the boundary enclosing the domain also gets discritised depending on the number of elements. Along a typical boundary element, displacement and normal rotations can be expressed as :

$$\begin{Bmatrix} w \\ \theta_x \\ \theta_y \end{Bmatrix} = \sum_{i=1}^{3} \begin{bmatrix} N_i^b & 0 & 0 \\ 0 & -N_i^b & 0 \\ 0 & 0 & -N_i^b \end{bmatrix} \begin{Bmatrix} w_i^b \\ \psi_{xi}^b \\ \psi_{yi}^e \end{Bmatrix} \tag{2.23}$$

or

$$\{u\} = \sum_{i=1}^{3} [N_i]^b \{a_i\}^b$$

where N_i^b represent one-dimensional shape functions.

The curvature vector can be written as

$$\begin{Bmatrix} \frac{\partial \theta_x}{\partial x} \\ \frac{\partial \theta_y}{\partial y} \\ \frac{\partial \theta_x}{\partial y} + \frac{\partial \theta_y}{\partial x} \end{Bmatrix} = \sum_{i=1}^{8} \begin{bmatrix} 0 & -N_{i,x}^e & 0 \\ 0 & 0 & -N_{i,y}^e \\ 0 & -N_{i,y}^e & -N_{i,x}^e \end{bmatrix} \begin{Bmatrix} w_i^e \\ \psi_{xi}^e \\ \psi_{yi}^e \end{Bmatrix} \tag{2.24}$$

or

$$\{\chi\} = \sum_{i=1}^{8} [B]_{bi}^e \{a_i\}^e$$

The shear strains can be written as

$$\begin{Bmatrix} \theta_x + \frac{\partial w}{\partial x} \\ \theta_y + \frac{\partial w}{\partial y} \end{Bmatrix} = \sum_{i=1}^{8} \begin{bmatrix} N_{i,x}^e & -N_i^e & 0 \\ N_{i,y}^e & 0 & -N_i^e \end{bmatrix} \begin{Bmatrix} w_i^e \\ \psi_{xi}^e \\ \psi_{yi}^e \end{Bmatrix} \tag{2.25}$$

or

$$\{\epsilon\}_s = \sum_{i=1}^{8} [B]_{si}^e \{a_i\}^e$$

The rotation θ_n on boundary C_3 can be expressed as :

$$\theta_n = \theta_x n_x + \theta_y n_y = \sum_{i=1}^{3} \begin{bmatrix} 0 & -N_i^b n_x & -N_i^b n_y \end{bmatrix} \begin{Bmatrix} w_i^b \\ \psi_{xi}^b \\ \psi_{yi}^b \end{Bmatrix} \tag{2.26}$$

or

$$\theta_n = \sum_{i=1}^{3} \{a_i\}^{bT} \{B_{ni}\}^{b}.$$

Substituting equations (2.22), (2.23), (2.24), (2.25) and (2.26) in (2.20) we get the functional in terms of the unknown vectors $\{a_i\}^e$ and $\{a_i\}^b$

$$\pi = \frac{1}{2} \sum_{e=1}^{n_e} \sum_{i=1}^{8} \sum_{j=1}^{8} \{a_i\}^{eT} [K_{bij}]^e \{a_j\}^e + \frac{1}{2} \sum_{e=1}^{n_e} \sum_{i=1}^{8} \sum_{j=1}^{8} \{a_i\}^{eT} [K_{sij}]^e \{a_j\}^e - \sum_{e=1}^{n_e} \sum_{i=1}^{8} \{a_i\}^{eT} \{f_i\}^e - \sum_{b=1}^{nb_2} \sum_{i=1}^{3} \{a_i\}^{bT} \{f_i\}^{b_2} - \sum_{b=1}^{nb_3} \sum_{i=1}^{3} \{a_i\}^{bT} \{f_i\}^{b_3} \qquad (2.27)$$

where

$$\left[K_{bij}\right]^e = \int_{A_e} \left[B_{bi}\right]^{eT} \left[D_b\right] \left[B_{bj}\right]^e dA \quad \text{(bending stiffness matrix)}$$

$$\left[K_{sij}\right]^e = \int_{A_e} \left[B_{si}\right]^{eT} \left[D_s\right] \left[B_{sj}\right]^e dA \quad \text{(shear stiffness matrix)}$$

$$\left\{f_i\right\}^e = \int_{A_e} \left[N_i\right]^{eT} \{b\}\, dA \quad \text{(body force vector)} \qquad (2.28)$$

$$\left\{f_i\right\}^{b_2} = \int_{C_b} \left[N_i\right]^{bT} \{t\}\, dS \quad \text{(surface force vector on } C_2\text{)}$$

$$\left\{f_i\right\}^{b_3} = \int_{C_b} \left[B_{ni}\right]^{b} m_n^*\, dS \quad \text{(surface force vector on } C_3\text{)}$$

Here A_e is the area of a typical plate element, C_b is the length of a typical boundary element, n_e is the total number of plate elements, n_{b2} is the total number of boundary element on the part C_2 and n_{b3} is the total number of boundary element on part C_3 of the boundary.

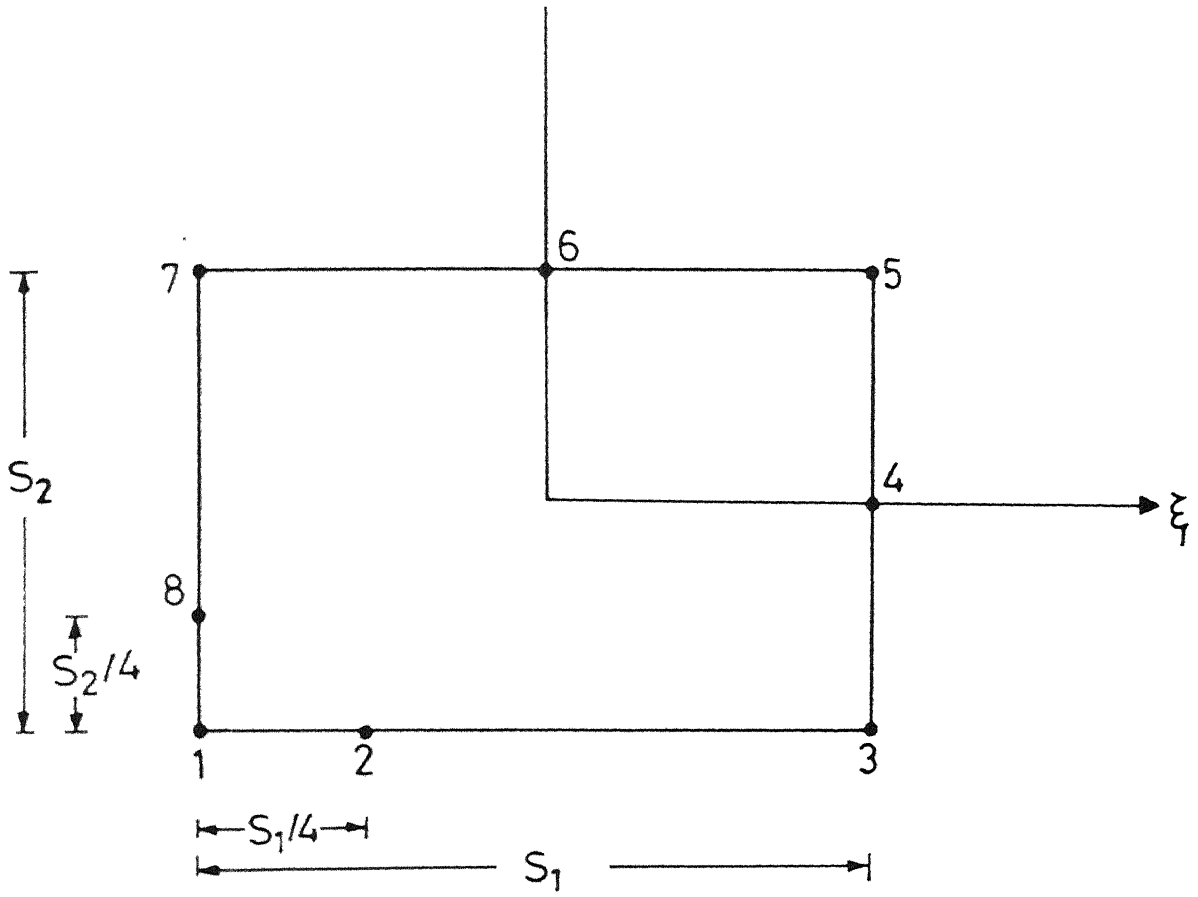

(a)

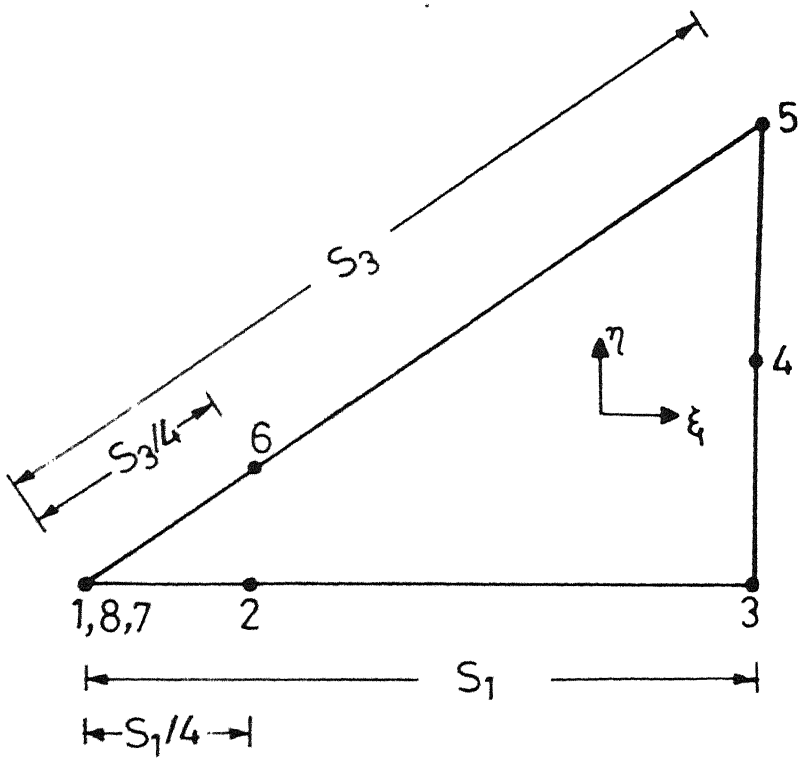

(b)

Fig 2.4

Using a standard procedure, the expression (2.27) for the total potential energy is expressed in terms of the global quantities in the following manner

$$\pi = \frac{1}{2} \{\Delta\}^T [K] \{\Delta\} - \{\Delta\}^T \{F\} \qquad (2.29)$$

Here [K] is the global stiffness matrix which contains the sum of expanded versions of both $\left[K_{bij}\right]^e$ and $\left[K_{sij}\right]^e$ over all the plate elements. Similarly the global force vector {F} contains the sum of expanded versions of all the three vectors $\{f_i\}^e$, $\{f_i\}^{b_2}$ and $\{f_i\}^{b_3}$ over appropriate plate and boundary elements. The vector {Δ} is called global displacement vector which contains the nodal values of w, θ_x and θ_y at all the nodes. When the plate is in equilibrium, π takes the minimum value. Minimisation of π with respect to {Δ} leads to the following algebraic equation

$$[K] \{\Delta\} = \{F\} \qquad (2.30)$$

At the crack tip stresses and strains are singular and they vary as inverse square root of the radial distance from the crack tip. If regular elements with biquadratic approximation for w, θ_x and θ_y are used to model the crack tip, then to get accurate stresses many such elements are required. There exist special crack tip elements which can model $1/\sqrt{r}$ singularity of stresses and strains at the crack tip. Accurate results are obtained by using four such elements at the crack tip. By placing mid side nodes at quarter point (Fig. 2.4(a)), $1/\sqrt{r}$ singularity of the strains and stresses is obtained only along the sides 1-2-3 and 1-8-7. If, additionally the side 1-8-7 is collapsed and node 6 is moved to the quarter point position (Fig. 2.4(b)), then this produces $1/\sqrt{r}$ singularity in every direction.

2.2.2 Evaluation of the stiffness matrix and force vector

The first step in calculation of the elemental stiffness matrices $\left[K_{bij}\right]^e$ and $\left[K_{sij}\right]^e$ is the evaluation of matrices $\left[B_{bi}\right]^e$ and $\left[B_{si}\right]^e$. This involves differentiation of shape functions N_i^e with respect to co-ordinates (x,y). This is done by using the chain rule :

$$N^e_{i,x} = N^e_{i,\xi}\ \xi_{,x} + N^e_{1,\eta}\ \eta_{,x}$$

$$N^e_{i,y} = N^e_{i,\xi}\ \xi_{,y} + N^e_{i,\eta}\ \eta_{,y} \qquad (2.31)$$

The derivatives of (ξ,η) coordinates with respect to (x,y) coordinates are evaluated from following transformation:

$$x = x(\xi,\eta)$$

$$y = y(\xi,\eta) \qquad (2.32)$$

For isoparametric elements this transformation is given by

$$\begin{Bmatrix} x \\ y \end{Bmatrix} = \sum_{i=1}^{8} \begin{bmatrix} N_i^e & 0 \\ 0 & N_i^e \end{bmatrix} \begin{Bmatrix} x_i^e \\ y_i^e \end{Bmatrix} \qquad (2.33)$$

where $(x_i^e,\ y_i^e)$ are the nodal values and N_i^e are the same shape functions as used in the interpolation of w, θ_x and θ_y (eqn. (2.21)). The Jacobian matrix of the transformation is given by

$$[J] = \begin{bmatrix} \partial x/\partial\xi & \partial y/\partial\xi \\ \partial x/\partial\eta & \partial y/\partial\eta \end{bmatrix} \qquad (2.34)$$

$$= \begin{bmatrix} \sum_{i=1}^{8} N^e_{i,\xi}\, x^e_i & \sum_{i=1}^{8} N^e_{i,\xi}\, y^e_i \\ \sum_{i=1}^{8} N^e_{i,\eta}\, x^e_i & \sum_{i=1}^{8} N^e_{i,\eta} y^e_i \end{bmatrix}$$

The derivatives $\xi_{,x}$, $\xi_{,y}$, $\eta_{,x}$ and $\eta_{,y}$ can now be obtained in the matrix from as

$$\begin{bmatrix} \xi_{,x} & \eta_{,x} \\ \xi_{,y} & \eta_{,y} \end{bmatrix} = [J]^{-1} \tag{2.35}$$

The integrals defining the elemental matrices $\left[K_{bij}\right]^e$ and $\left[K_{sij}\right]^e$ and the elemental vectors $\{f_i\}^e$, $\{f_i\}^{b_2}$ and $\{f_i\}^{b_3}$ are evaluated numerically by Gauss-Legendre numerical integration formulas. For that purpose, the variables of integration need to be transformed from (x,y) to (ξ,η). When this is done the integrals become

$$\begin{aligned}
\left[K_{bi}\right]^e &= \int_{-1}^{+1}\int_{-1}^{+1} \left[B_{bi}\right]^{eT} [D]_b \left[D_{bi}\right]^e \det [J]\, d\xi\, d\eta \\
\left[K_{si}\right]^e &= \int_{-1}^{+1}\int_{-1}^{+1} \left[B_{si}\right]^{eT} [D]_s \left[B_{bi}\right]^e \det [J]\, d\xi\, d\eta \\
\left\{f_i\right\}^e &= \int_{-1}^{+1}\int_{-1}^{+1} \left[N_i\right]^{eT} [b] \det [J]\, d\xi\, d\eta \qquad (2.36) \\
\left\{f_i\right\}^{b_2} &= \int_{-1}^{+1} \left[N_i\right]^{bt} [t]^T \frac{ds}{d\xi}\, d\xi \\
\left\{f_i\right\}^{b_3} &= \int_{-1}^{+1} \left[B_{ni}\right]^b m^*_n \frac{ds}{d\xi}\, d\xi .
\end{aligned}$$

The derivative $\frac{ds}{d\xi}$ is evaluated by using the transformation between the global boundary coordinate s and the local boundary coordinate

ζ which is consistent with transformation (2.33).

The requirement of only C^0 continuity of displacements and independent rotations in the Mindlin formulation allows the use of a wide range of interpolation schemes. However, when exact numerical integration scheme is used for thin plates with standard Mindlin finite elements, the stiffness matrix becomes very large leading to inaccurate results. This phenomenon, which is termed locking, is caused by the imposition of the constraints $\gamma_{xz} = \gamma_{yz} = 0$ in the shear strain energy terms for thin plates. The part of the stiffness matrix corresponding to transverse shear strain energy may be interpreted as penalty functions which force the shear strains to become zero as the plate thickness-to-span ratio is reduced.

When a reduced order of numerical integration of the stiffness terms is used on some isoparametric Mindlin plate elements improved behaviour is often obtained. The use of reduced integration, though successful in some cases, produces the further problem of rank deficiency of the stiffness matrix. In selective integration approach reduced integration rule is used only for the stiffness matrix associated with the transverse shear strain energy. This is done to alleviate the overconstraining effects of this portion of stiffness matrix. Full integration is used on the remaining terms in an attempt to retain the required rank of the overall stiffness matrix. Fig. 2.5 shows the exact, reduced and selective integration rules used for typical serendipity and Lagrangian mindlin plate elements.

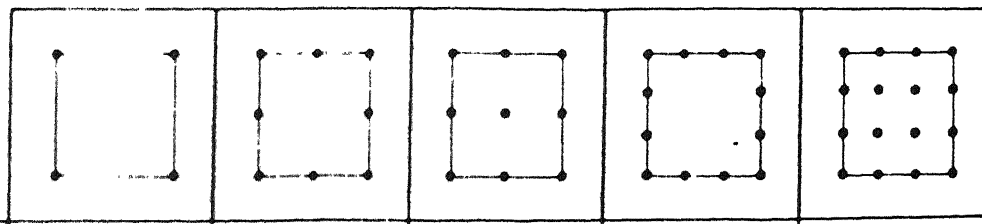

Shape functions Formulation	Linear Langrangian	Quadratic Serendipity	Quadratic Langrangian	Cubic Serendipity	Cubic Lagrangian
Full integration	2 x 2 LF1	3 x 3 SF2	3 x 3 LF2	4 x 4 SF3	4 x 4 LF3
Reduced integration	1 x 1 LR1	2 x 2 SR2	2 x 2 LR2	3 x 3 SR3	3 x 3 LR3
Selective integration	shear 1 x 1 bending 2 x 2 LS1	2 x 2 3 x 3 SS2	2 x 2 3 x 3 LS2	3 x 3 4 x 4 SS3	3 x 3 4 x 4 LS3

Fig. 2.5 Reduced and Selective integration schemes

Global assembly of elemental matrices $\left[K_{bij}\right]^e$ and $\left[K_{sij}\right]^e$ to [K] and of element force vector $\{f_i\}^e$, $\{f_i\}^{b_2}$ and $\{f_i\}^{b_3}$ into {F}, and application of essential boundary conditions on part C_1 and C_3 is done using standard procedures.

2.2.3 Post Processing and Stress Intensity Factor

The set of equations resulting after application of boundary conditions are solved using Frontal Solver. On solving these equations values of w, θ_x and θ_y are obtained. Further, curvatures, bending moment and shear forces are evaluated at gauss points.

In plate bending problems when the distributed moments $\tilde{m}_x$ and $\tilde{m}_y$ are absent certain Path independent integrals are used in the prediction of crack initiation. When x-axis is taken along the crack, these integrals are defined by

$$J_x = \int_\Gamma \left\{ (W - p_z w)\, n_x - \left[M_x \frac{\partial \theta_x}{\partial x} + M_{xy} \frac{\partial \theta_y}{\partial x} + Q_x \frac{\partial w}{\partial x} \right] n_x - \left[M_{xy} \frac{\partial \theta_x}{\partial x} + M_y \frac{\partial \theta_y}{\partial x} + Q_y \frac{\partial w}{\partial x} \right] n_y \right\} d\Gamma - \int_\Omega \frac{\partial p_z}{\partial x} w \, d\Omega \tag{2.37}$$

$$J_y = \int_\Gamma \left\{ (W - p_z w)\, n_y - \left[M_x \frac{\partial \theta_x}{\partial y} + M_{xy} \frac{\partial \theta_y}{\partial y} + Q_x \frac{\partial w}{\partial y} \right] n_x - \left[M_{xy} \frac{\partial \theta_x}{\partial y} + M_y \frac{\partial \theta_y}{\partial y} + Q_y \frac{\partial w}{\partial y} \right] n_y \right\} d\Gamma - \int_\Omega \frac{\partial p_z}{\partial x} w \, d\Omega - \int_{\Gamma_1} \left[W - p_z w \right] n_x \, d\Gamma \tag{2.38}$$

where

W = strain energy density

$\left[W\ p_z w\right]$ = discontinuity (or jump) across the crack surfaces.

Γ = Path extending along the upper and lower crack surfaces.

Ω = domain enclosed by curve Γ

$\hat{n}$ = outward drawn normal

J_x can be broken into shear and bending part, such that

$$J_x = J_x^B + J_x^s \tag{2.39}$$

where

$$J_x^B = \int_\Gamma \left[W^b\, n_x - \left(M_x \frac{\partial \theta_x}{\partial x} + M_{xy} \frac{\partial \theta_y}{\partial x}\right) n_x \left(M_{xy} \frac{\partial \theta_x}{\partial x} + M_y \frac{\partial \theta_y}{\partial x}\right) n_y\right] d\Gamma$$

$$+\int_\Omega \left(Q_x \frac{\partial \theta_x}{\partial x} + Q_y \frac{\partial \theta_y}{\partial x}\right) d\Omega \tag{2.40}$$

$$J_x^s = \int_\Gamma \left[\left(W^s - P_{zw}\right) n_x - \left(Q_x\, n_x + Q_y\, n_y\right) \frac{\partial w}{\partial x}\right] d\Gamma - \int_\Omega \left(Q_x \frac{\partial \theta_x}{\partial x} + Q_y \frac{\partial \theta_y}{\partial x}\right) d\Omega$$

The stress intensity factors are defined by the relations

$$K_1 = \lim_{r \to 0} \sqrt{2r}\ M_{yy}(r,0)$$

$$K_2 = \lim_{r \to 0} \sqrt{2r}\ M_{xy}(r,0) \tag{2.41}$$

$$K_3 = \lim_{r \to 0} \sqrt{2r}\ Q_x(r,0)$$

In the elastic case the stress intensity factors K_1, K_2 and K_3 are related to J_x^B, J_x^s and J_y as

$$J_x^B = \frac{12\pi}{Eh^3}\left[K_1^2 + K_2^2\right] \tag{2.42}$$

$$J_x^s = \frac{6(1+\nu)\pi}{5Eh} K_3^2 \tag{2.43}$$

$$J_y = -\frac{24\pi}{Eh^3} K_1 K_2 \tag{2.44}$$

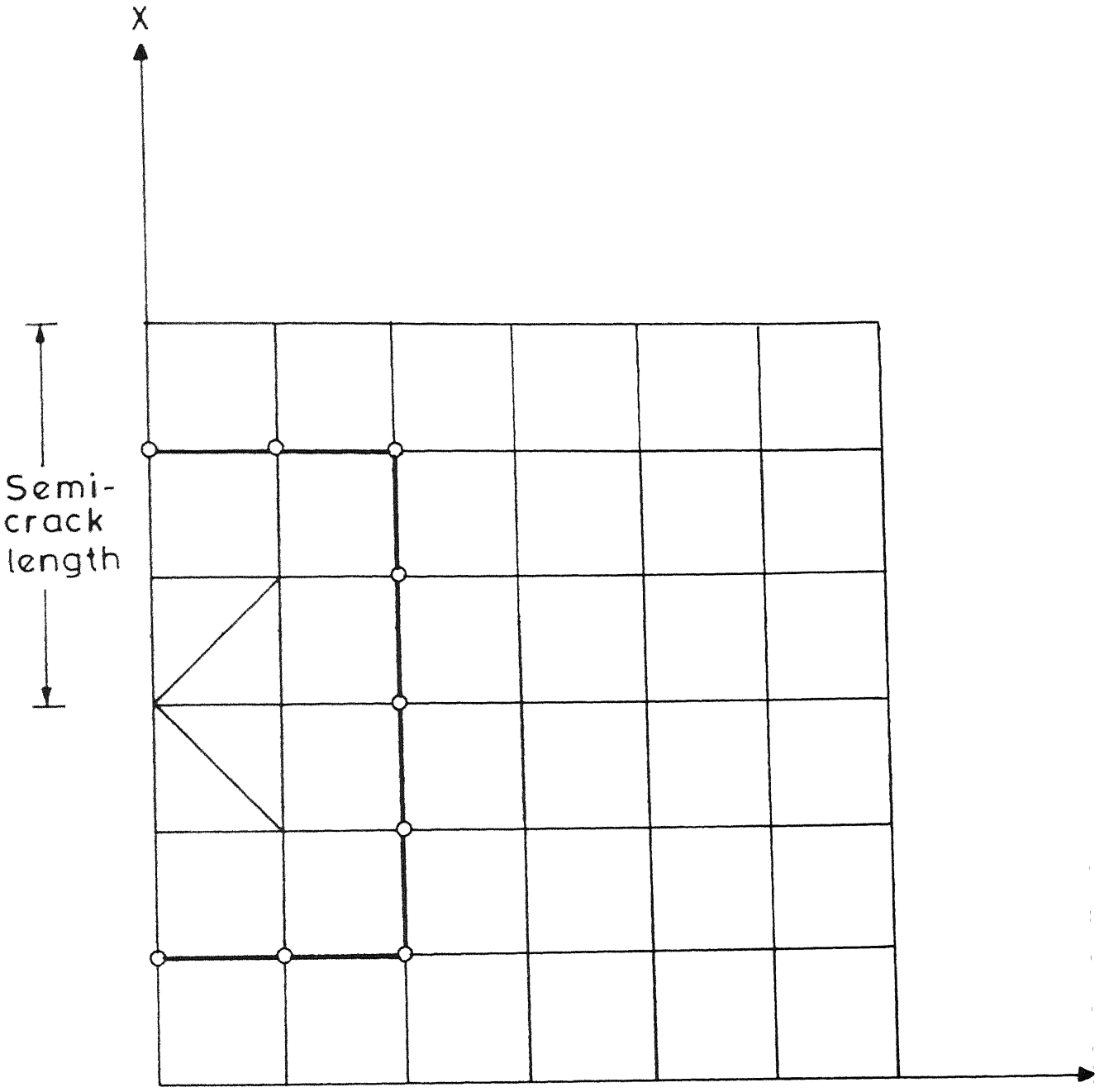

Fig. 2·6

on combining (2.42) and (2.43)

$$J_x = J_x^B + J_x^s = \frac{12\pi}{Eh^3}\left[K_1^2 + K_2^2 + \frac{h^2}{10}(1+\nu)K_3^2\right] \qquad (2.45)$$

As the domain under consideration is subjected to Uniform transverse load and the geometry and boundary conditions are symmetric only K_1 is dominant and K_2, K_3 are negligible. Therefore K_1 is evaluated from J_x by setting K_2 and K_3 to zero in equation (2.45). In the present study crack is either parallel or perpendicular to the fixed supports. Since x-axis is along the crack in the definition of J_x, the direction of x axis in the two cases is different. The typical mesh and path of integration are shown in Fig. 2.6.

CHAPTER III

RESULTS & DISCUSSIONS

In this chapter the Mindlin finite element formulation developed in Chapter II has been applied to a part of submarine hull subjected to uniform transverse load. To check the software package results obtained by the same are compared with test problems at various stages. The variation of the stress intensity factor in mode I is studied with respect to the crack length, the plate length, the plate thickness, the crack orientation and the boundary conditions.

3.1 Test Problems

Two test problems discussed by Hinton and Owen [19] are solved to check the basic software for an uncracked plate in pure bending based on Mindlin's plate theory. The results obtained were in complete agreement with those presented in [19].

3.1.1 Singular Elements

The problem of simply supported rectangular plate with a crack at the center is solved for the case of a uniform transverse load. Fig. 3.1 shows the domain and finite element model for a quarter of the plate. The total number of elements used in the model are 22 including four crack tip singular elements. The material properties of the plate are :

$$E = 10920 \frac{N}{mm^2} \quad \nu = 0.3$$

Fig. 3.2 shows transverse displacements at different sections of the plate as presented in reference [13]. Fig. 3.3 shows the

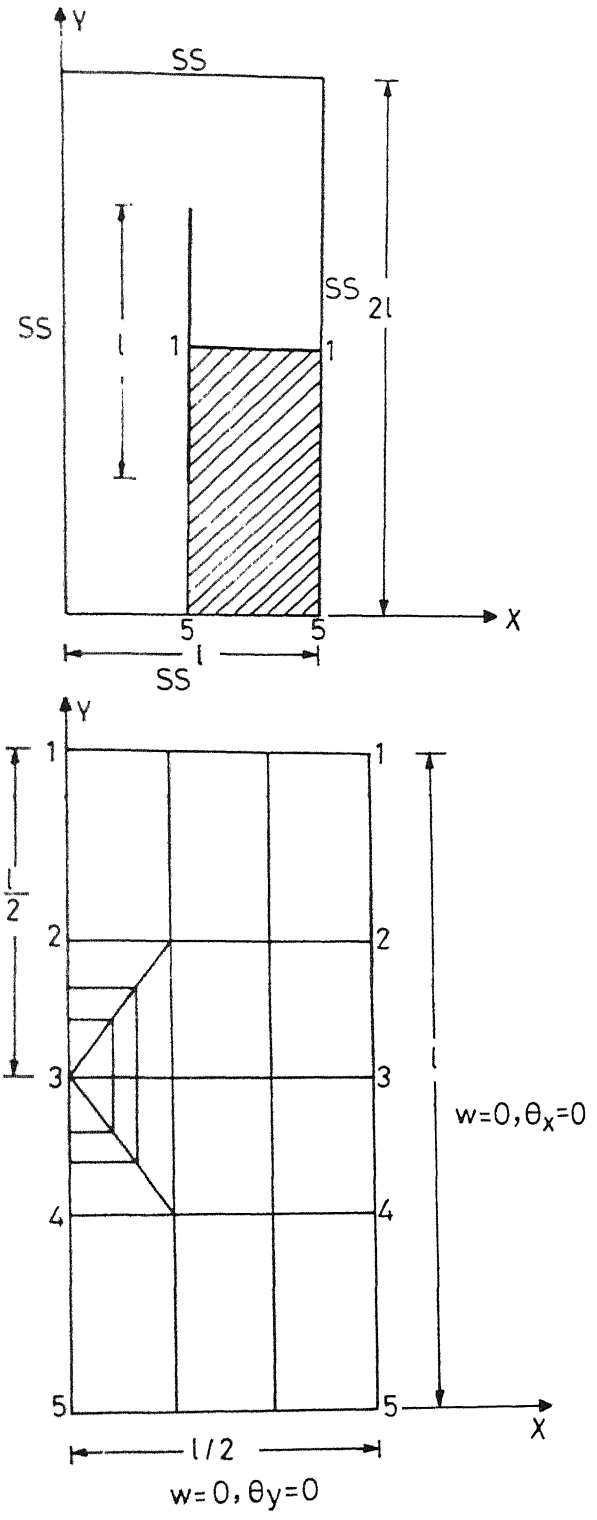

Fig.3·1 Test problem for singular elements

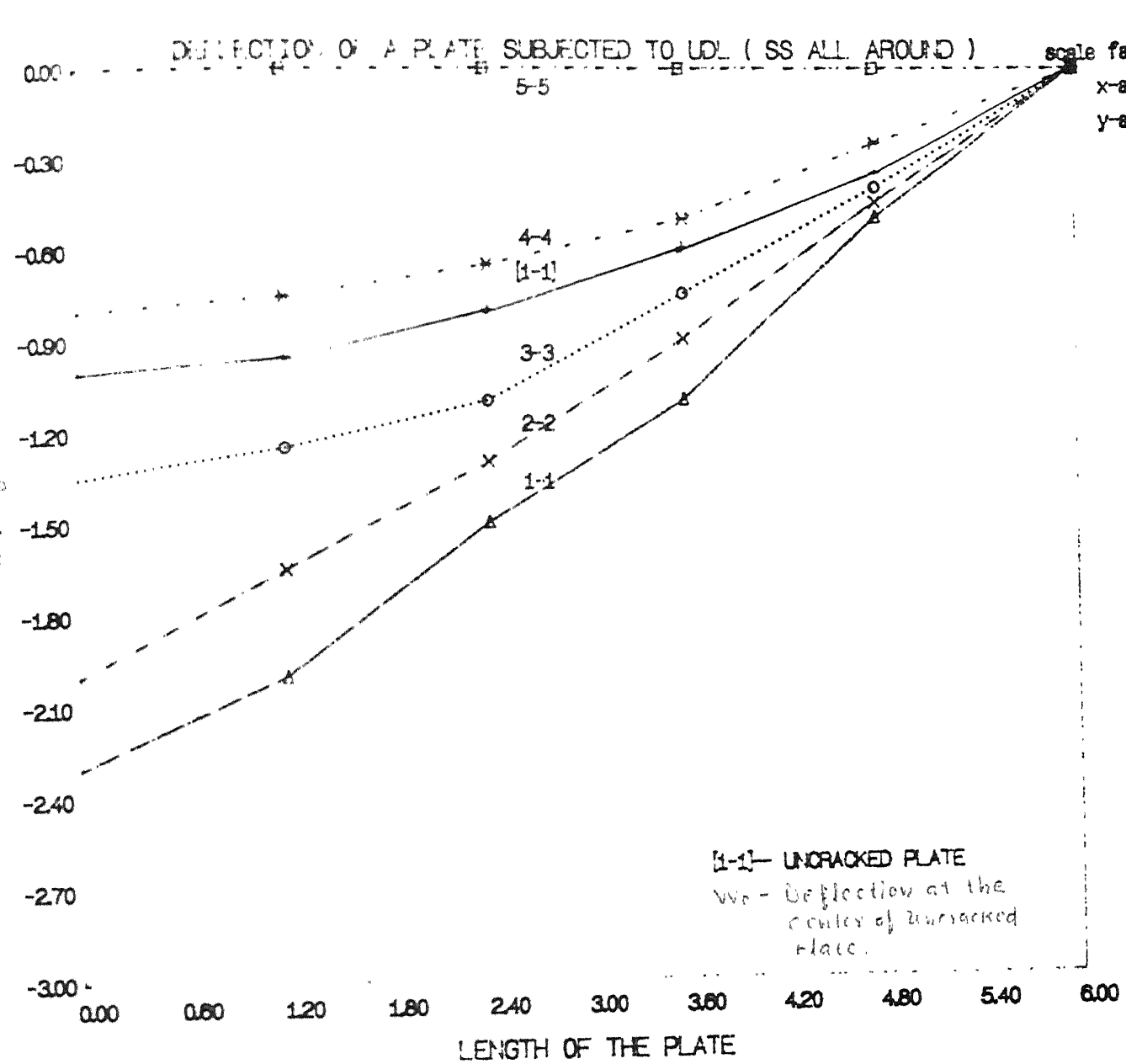

Fig. 3.2 Deflection of a rectangular cracked plate (Reference result)

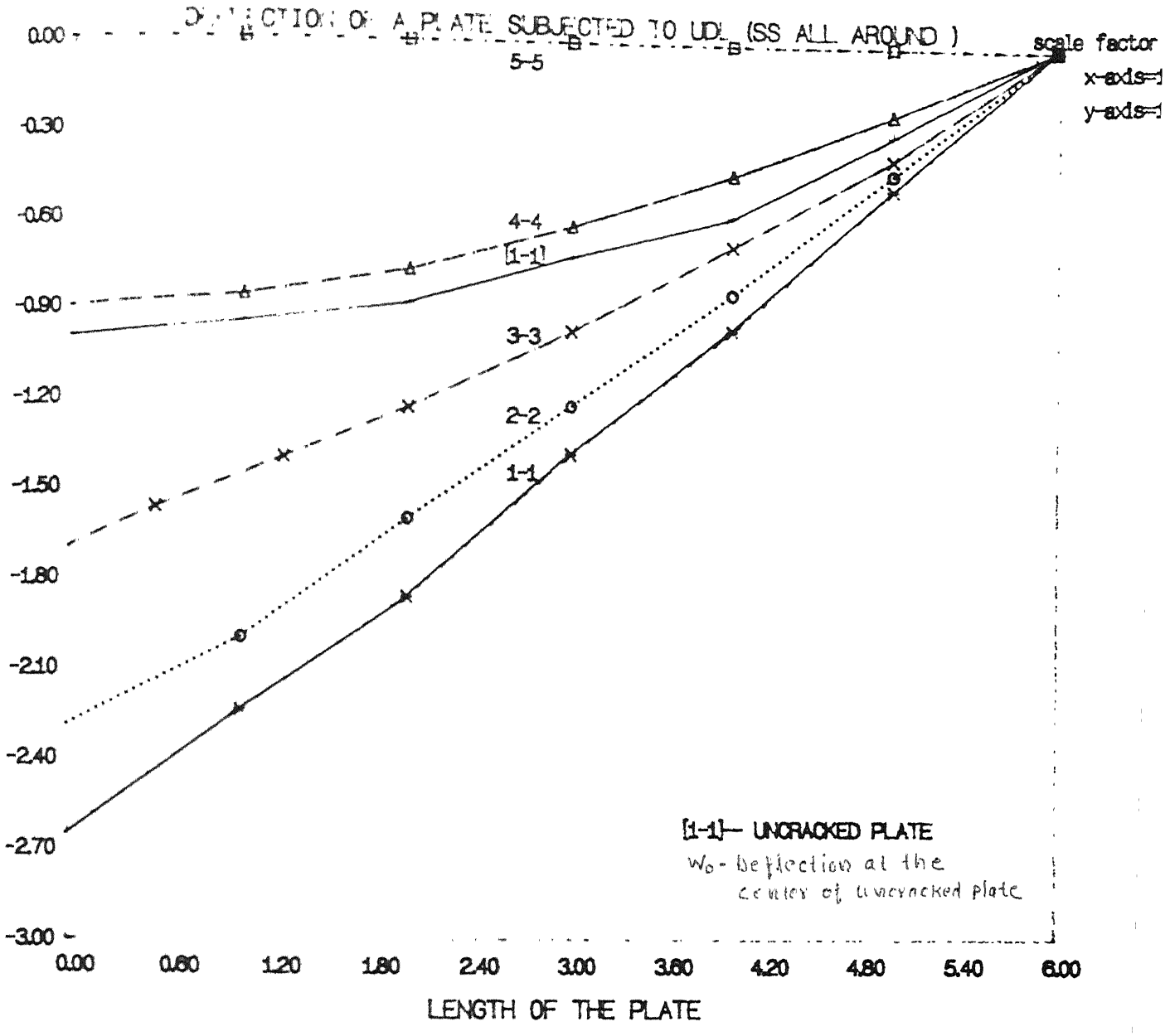

Fig. 3.3 Deflection of a rectangular cracked plate (Result obtained)

displacements obtained by the present model. It can be seen that the trends in the two figures match quite well. This shows that singular elements model behaviour of cracked plates quite well.

3.1.2 J integral and SIF

To verify the validity of J integral approach to determine the stress intensity factor a test problem is solved and the results are compared with those of Sosa and Eischen [15]. The domain is a square plate, simply supported all around and subjected to a uniform pressure load, as shown in Fig. 3.4. The finite element model contains 66 elements in a quarter of the plate. The material properties used :

$$E = 1000 \frac{N}{mm^2} \qquad \nu = 0.3$$

Fig. 3.5 shows the result from Reference [15], on the effects of crack length and plate thickness on the normalised stress intensity factor. The normalised stress intensity factor is defined as

$$\tilde{K}_1 = \frac{K_1}{P_z B^2 \sqrt{a}}$$

where

P_z = uniform transverse load

B = halt plate width

a = semi crack length

The results obtained by the present model are depicted in Fig. 3.6. It is observed that the trends and the values are in close agreement with those shown in Fig. 3.5. This problem validates the complete formulation presented in Chapter II and the software package developed.

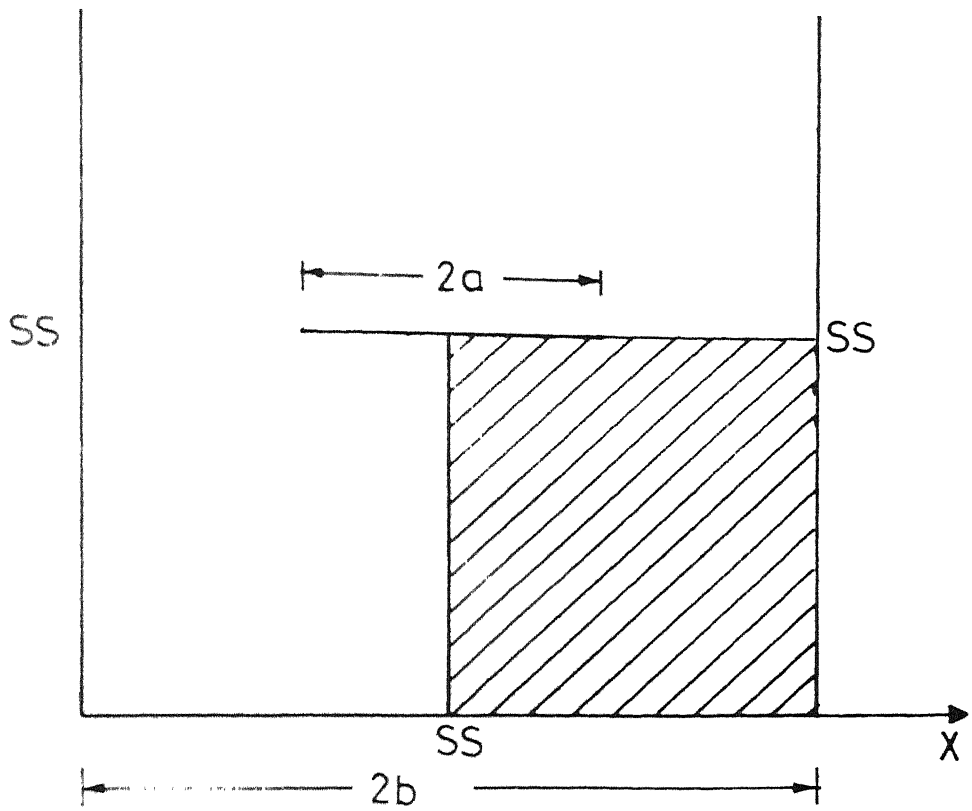

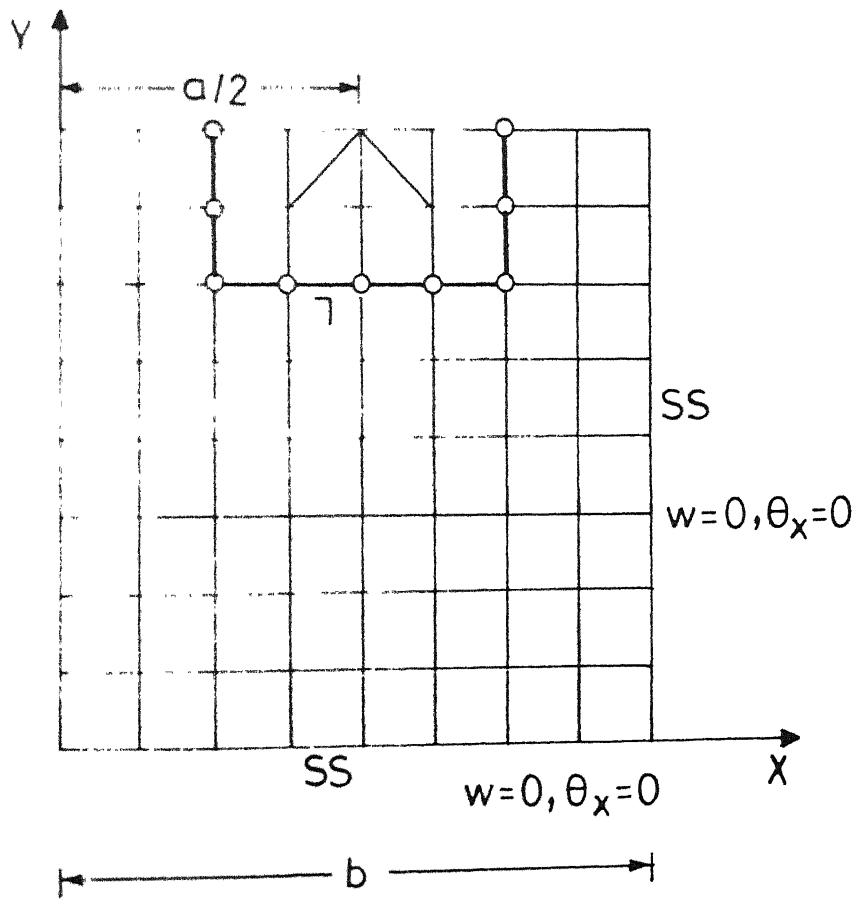

Fig. 3-4 Test problem (J integral)

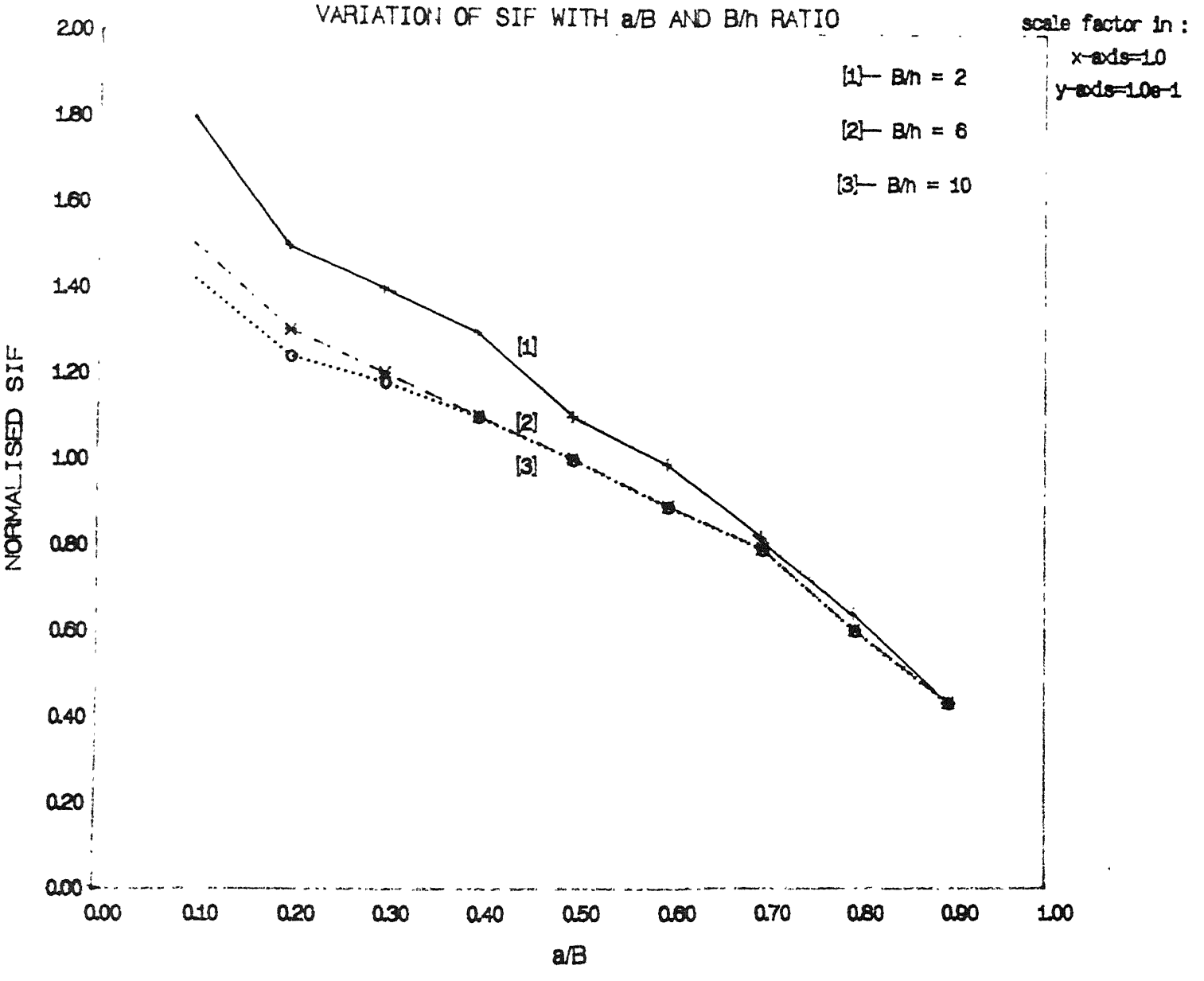

Fig. 3.5 Variation of Normalised SIF for a cracked Square Plate
(Reference Result)

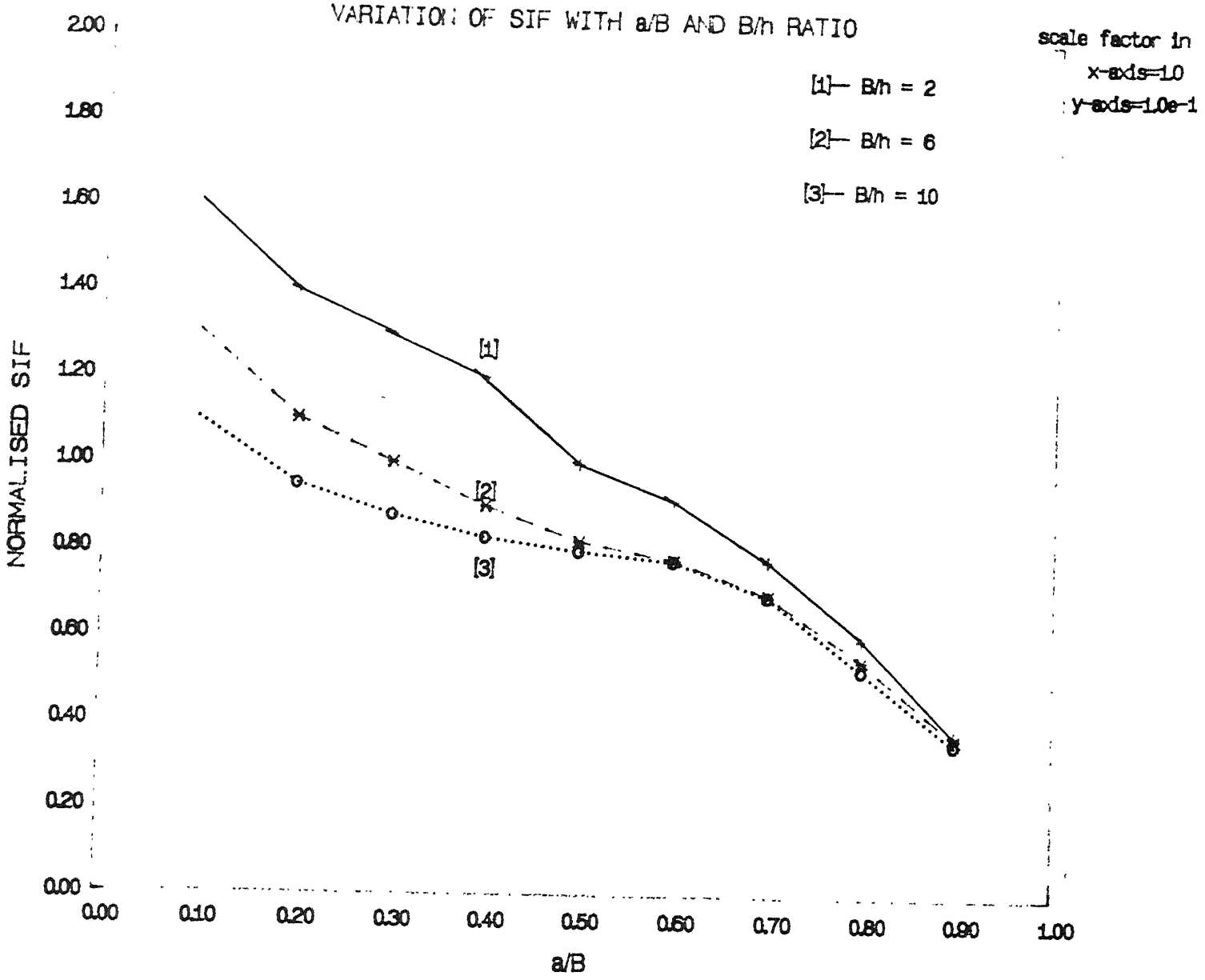

Fig. 3.6 Variation of Normalised SIF for a cracked Square Plate

(Result obtained)

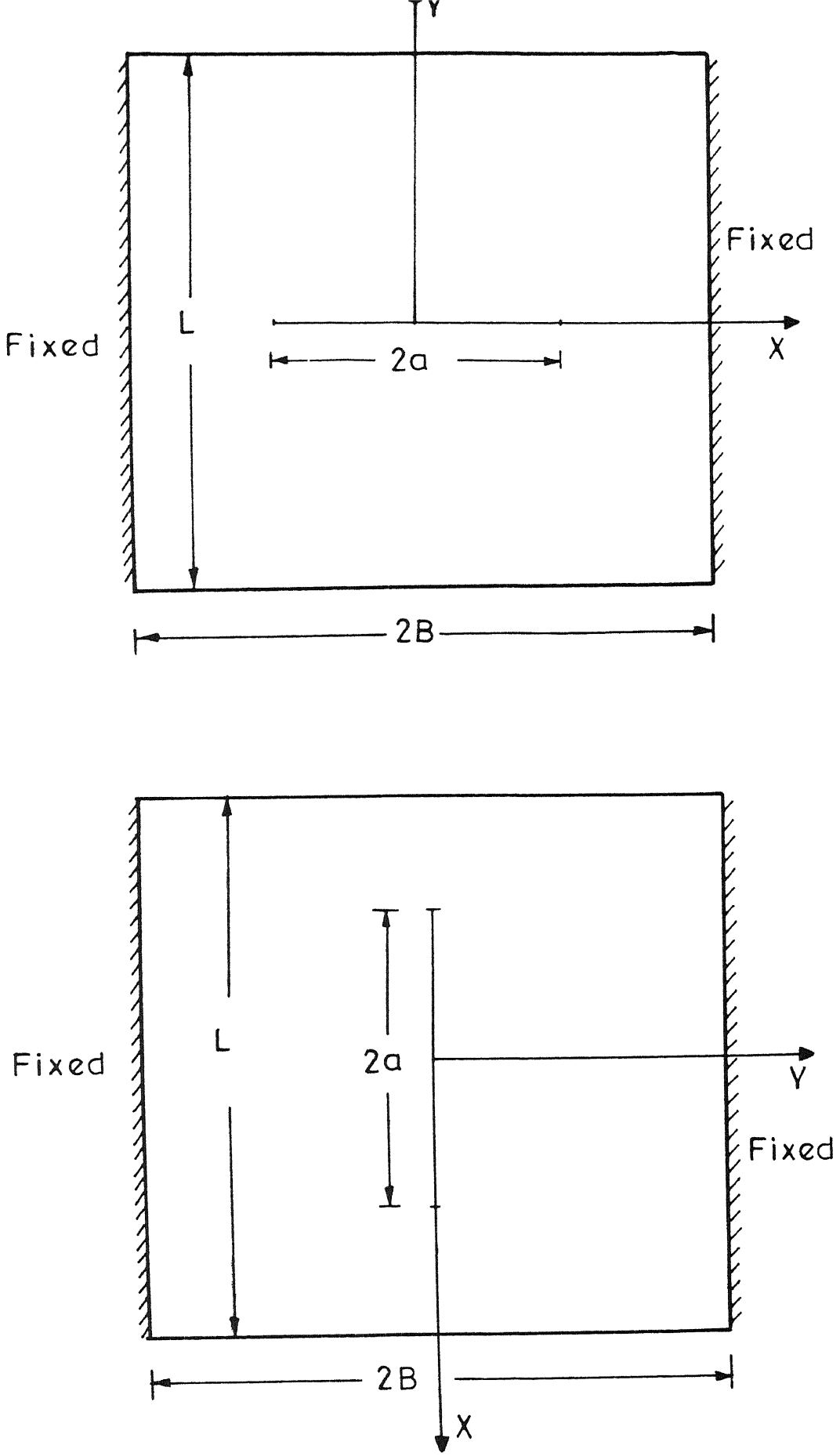

Fig. 3·7 Plate geometry and crack orientation

3.2 Parametric Studies

Submarine hull is fabricated by welding of plates on circumferential rings. One such plate mounted between two adjacent stiffening rings has been localised for analysis as shown in Fig. 3.7. The two ends welded on stiffening rings are idealised as fixed ends and the distance (2B) between them is assumed constant. As the boundary conditions at the other two edges do not fall in standard categories they are parametrically chosen as free and simply supported. The distance L between these two edges and the thickness h of the plate are varied to study their effects on the stress intensity factor. The crack is taken either parallel or perpendicular to the fixed supports (Fig. 3.7). The material properties used are :

$$E = 1000 \frac{N}{mm^2} \qquad \nu = 0.3$$

3.2.1 Simply Supported Case

(A) Crack Parallel to fixed supports

Normalised stress intensity factor is plotted as a function of a/B, for various h/B and L/B ratios in Fig. 3.8 and Fig. 3.9 respectively. The normalised stress intensity factor is defined as before. In an infinite plate containing a crack of length 2a and bent by uniform bending movement M_o applied at infinity, it is observed that the normalised SIF ($K_1/M_o \sqrt{a}$) increases with plate thickness h but decreases with the semi crack length 'a' (Hartrancraft and Sih [7], Viswanath et al [10]). In a finite plate also similar trends are observed by Viswanath et al [10] for the case of edge movements and by Sosa and Eischen [15] for the

case of uniform transverse load. This may be because the infinite plate solution for the bending moment distribution remains valid in the neighbourhood of a crack in finite plate as well. The trends exhibited by our results (Fig. 3.8) agree with those in above references. Note that although normalised SIF decreases with 'a', the dimensional SIF may not necessarily decrease with it as the expression for normalised SIF contains $\sqrt{a}$ in its denominator. Further it is observed that when the thickness to width ratio (h/B) is reduced beyond 0.02, there is hardly any change in the normalised SIF. In Kirchoff's thin plate theory, SIF does not depend on the plate thickness, so it can be concluded that the limiting h/B value upto which the thin plate theory is valid is approximately 0.02.

As the length (L) is increased it is observed that normalised SIF increases (Fig. 3.9). The stress intensity factor depends on the bending moment values in the vicinity of the crack. For a parallel crack these values are primarily affected by the reactions at fixed supports. However these reactions are influenced by the boundary conditions on other two edges as well. It is observed that beyond L/B = 2.0 normalised SIF is not significantly affected by these boundary conditions.

(B) Crack perpendicular to fixed supports

The trend of variation of normalised SIF with respect to h/B, L/B and a/B ratio is similar. However the values of normalised stress intensity factor are more in this case (Fig. 3.10 and Fig. 3.11). This happens because when the crack is perpendicular, the bending moment values in the neighbourhood of the crack are not

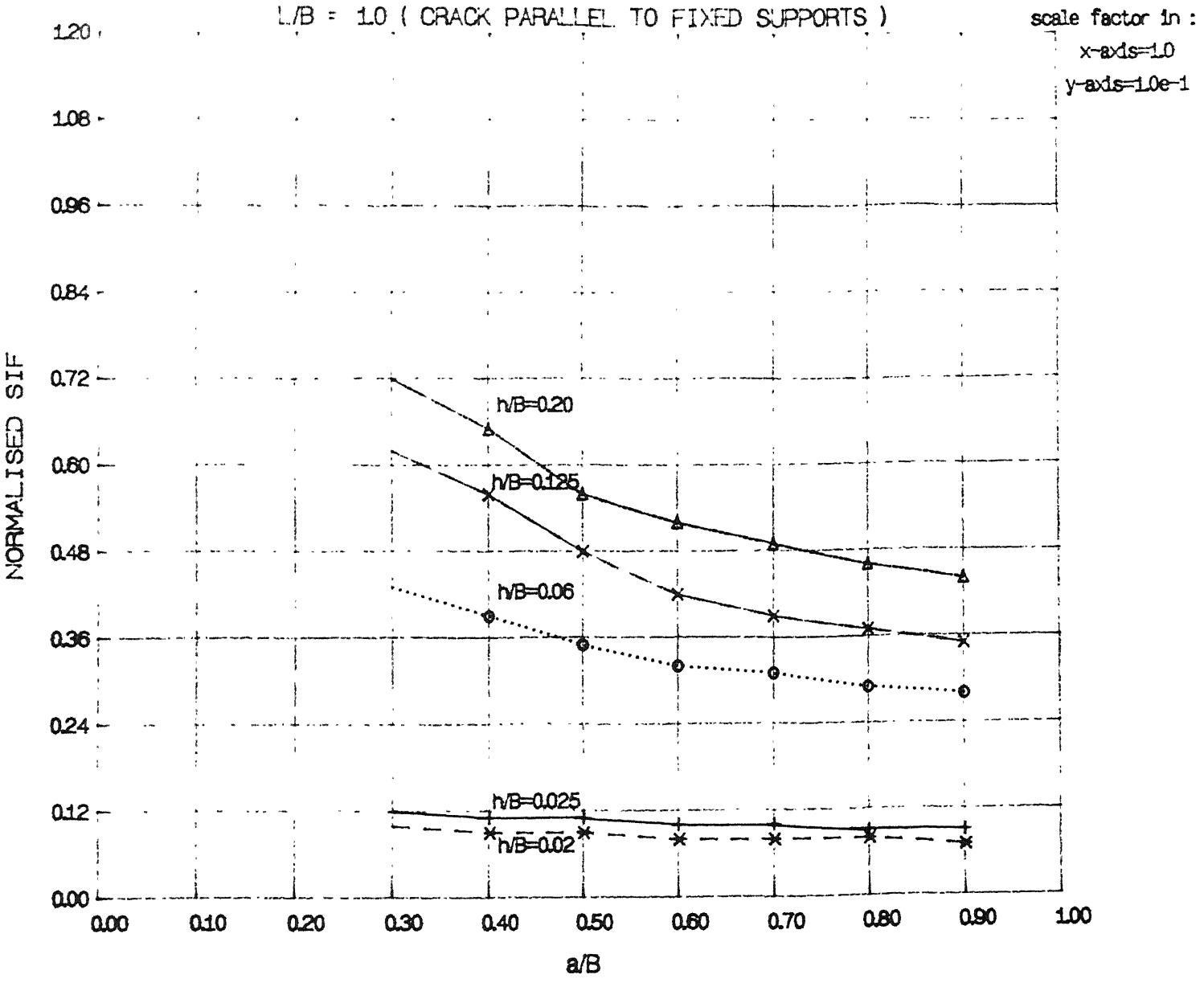

Fig. 3.8 Effect of h/B ratio on normalised SIF (Simply Supported ends)

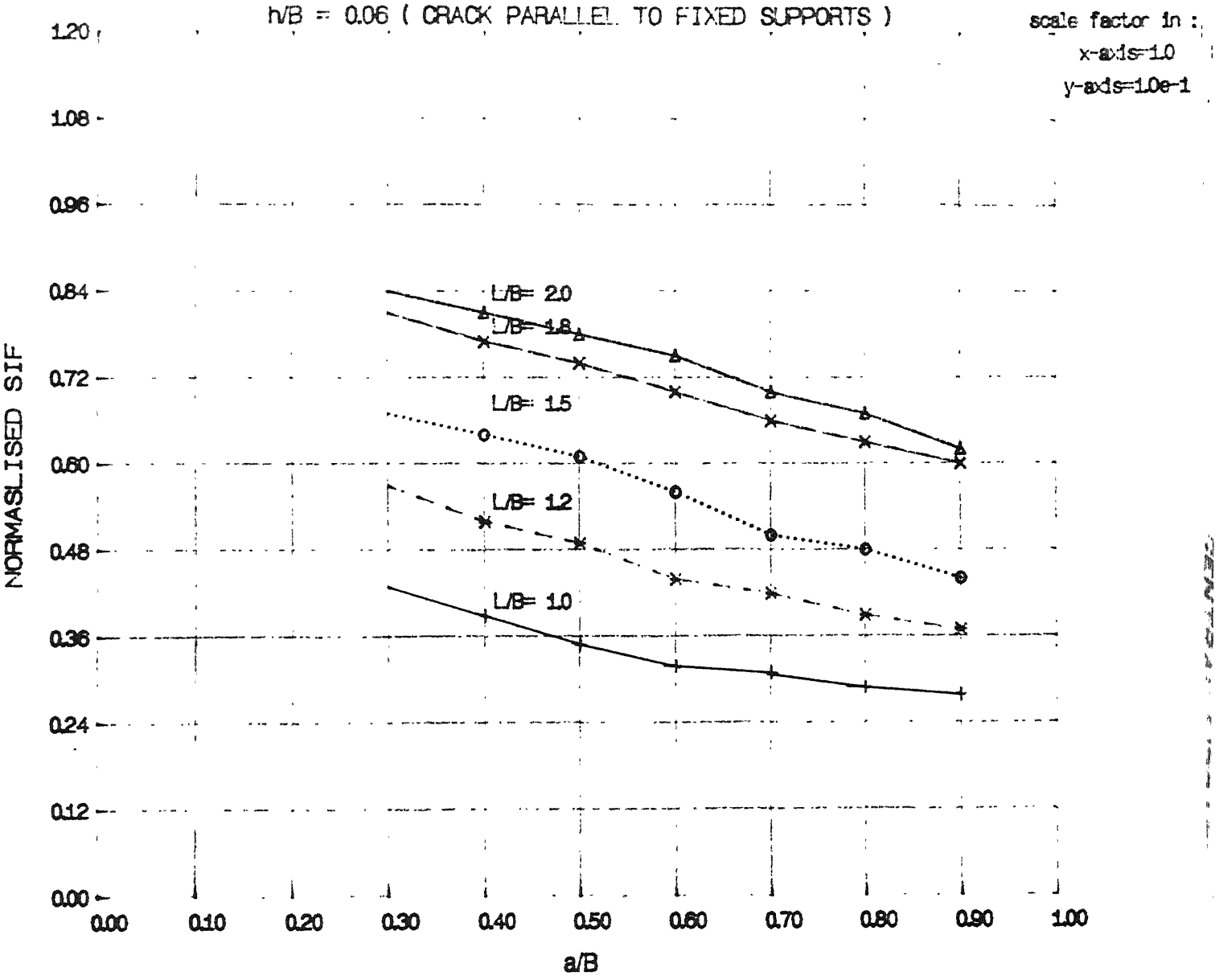

Fig. 3.9 Effect of L/B ratio on normalised SIF (simply supported ends)

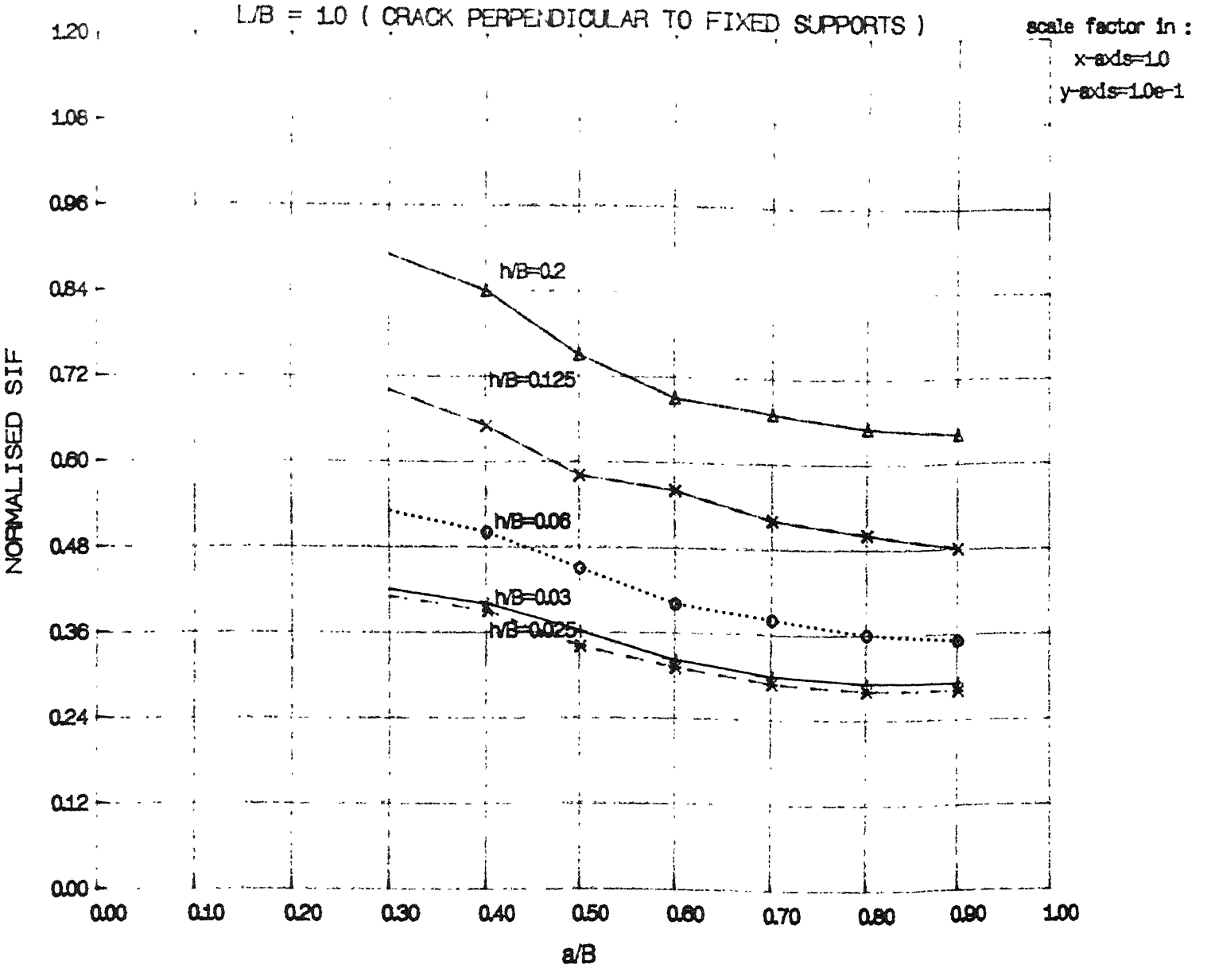

Fig. 3.10 Effect of h/B ratio on normalised SIF (simply supported ends)

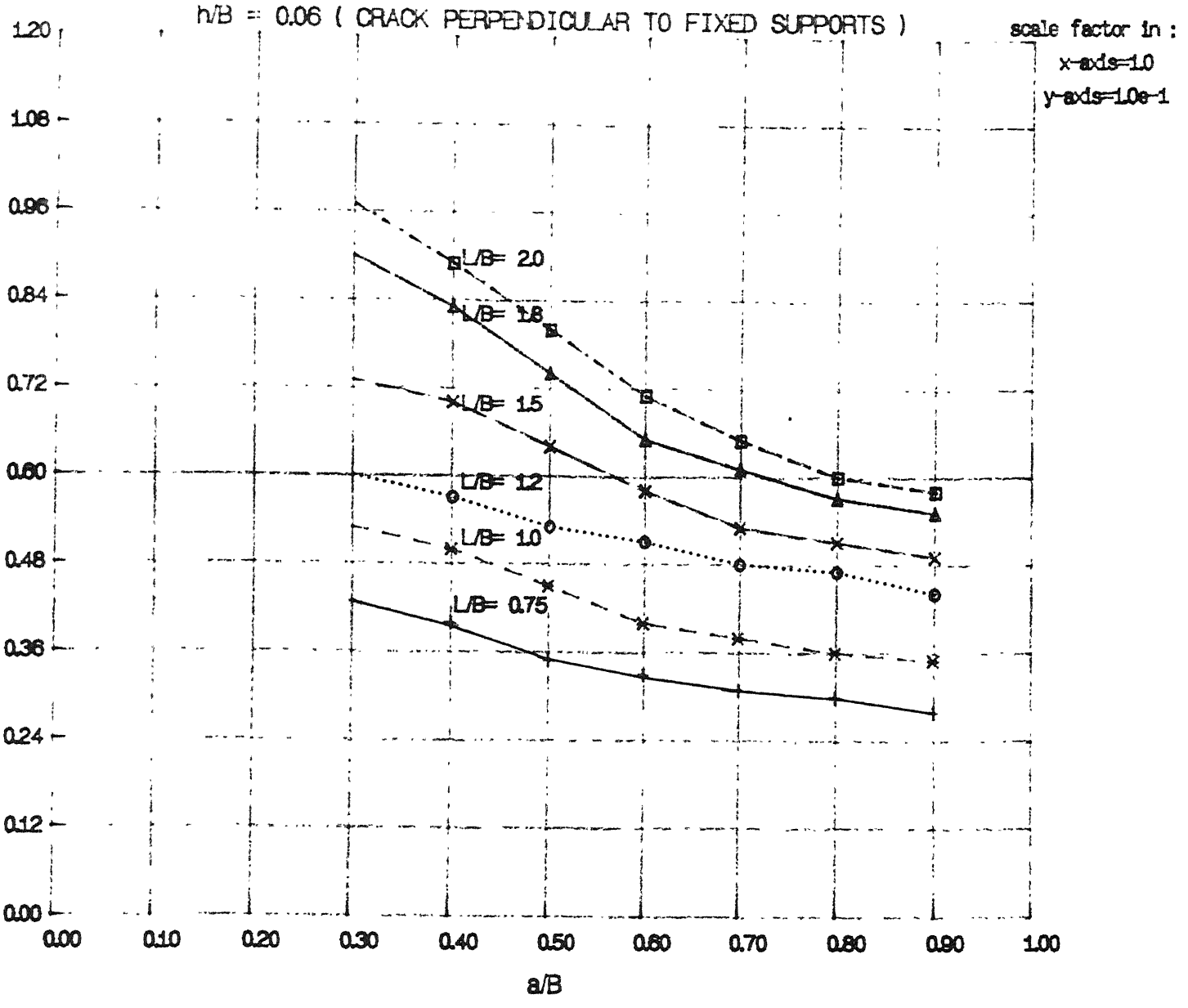

Fig. 3.11 Effect of L/B ratio on normalised SIF (simply supported ends)

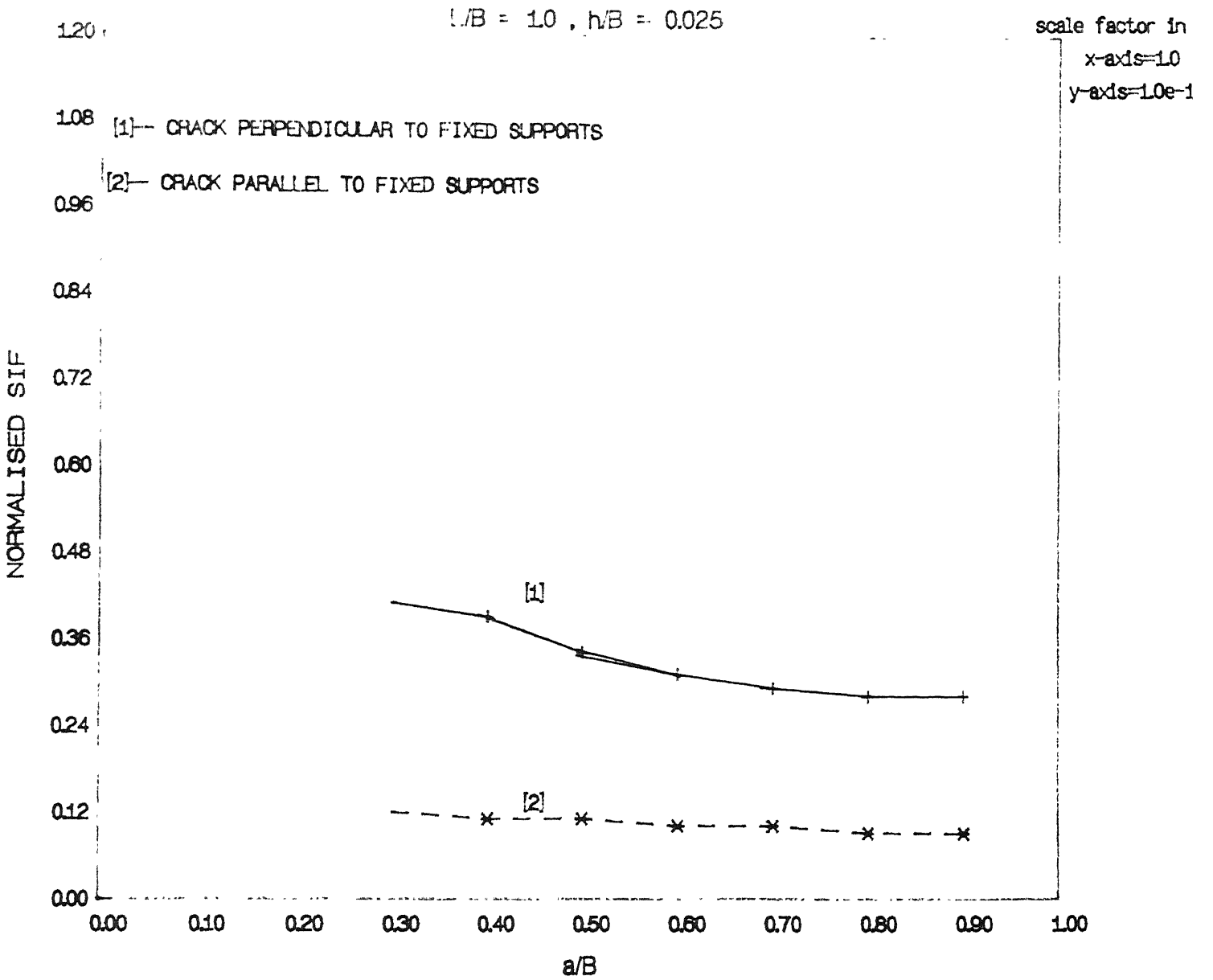

Fig. 3.12 Effect of crack orientation on normalised SIF (Simply Supported ends)

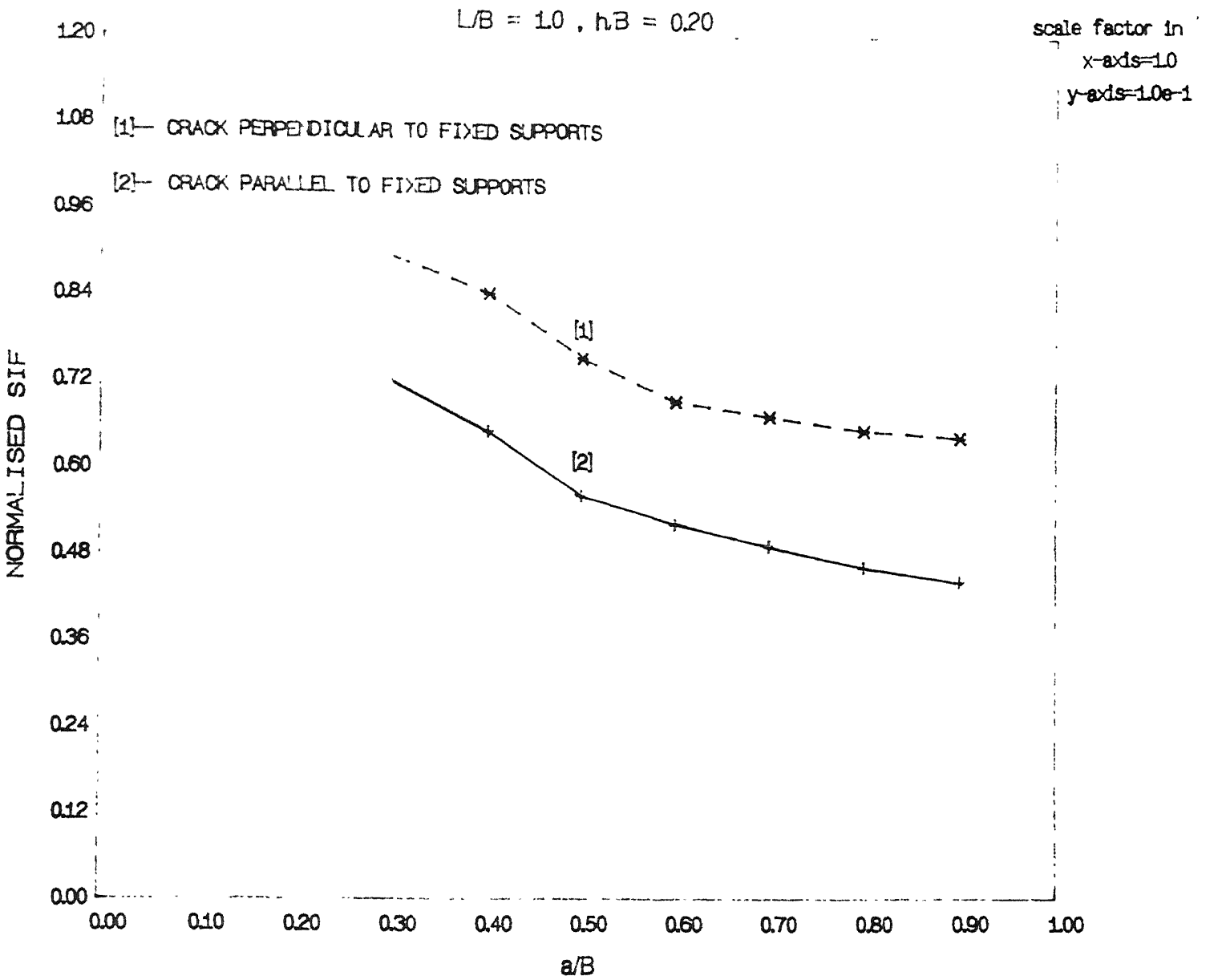

Fig. 3.13 Effect of crack orientation on normalised SIF (Simply Supported ends)

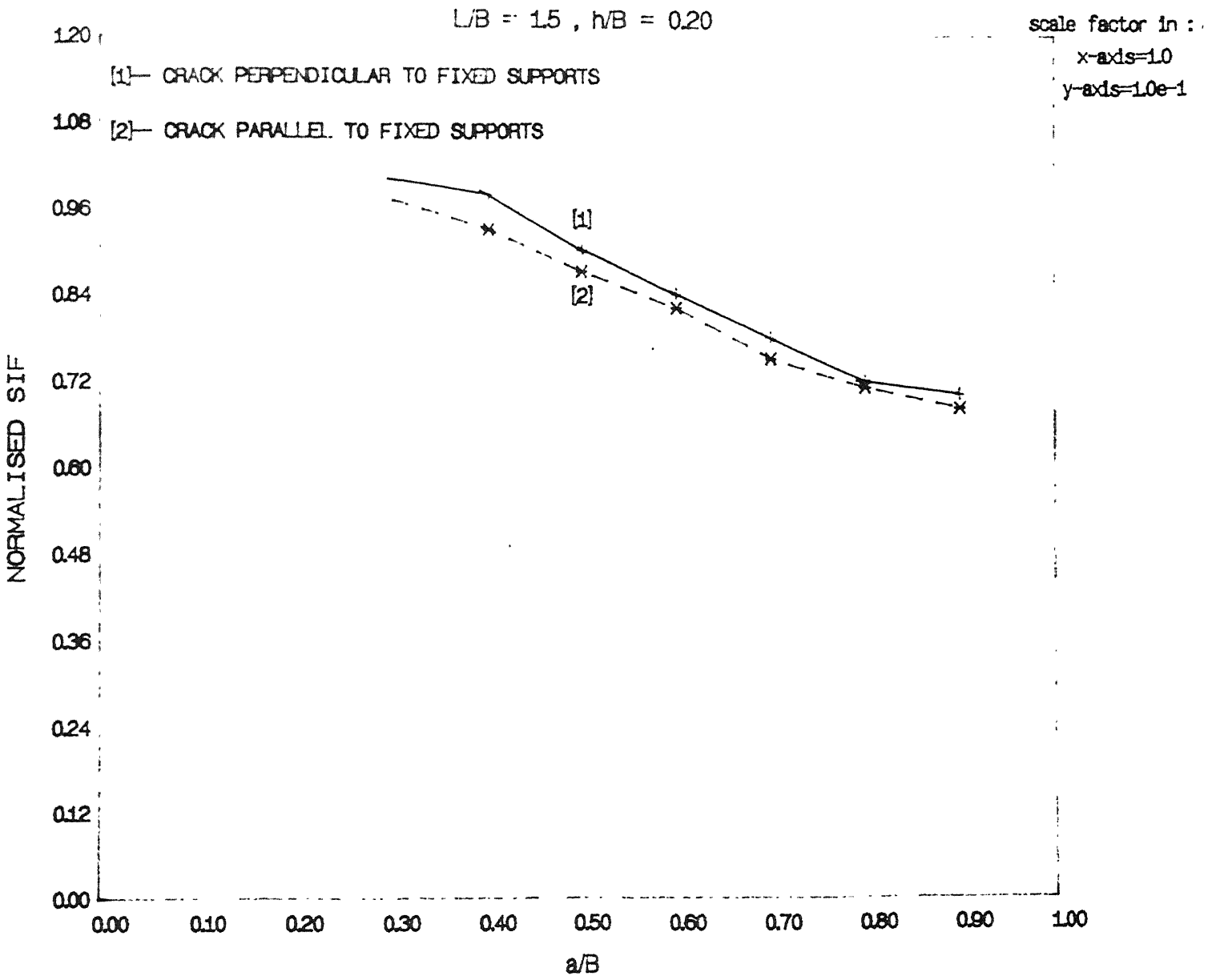

Fig. 3.15 Effect of crack orientation on normalised SIF (Simply Supported ends)

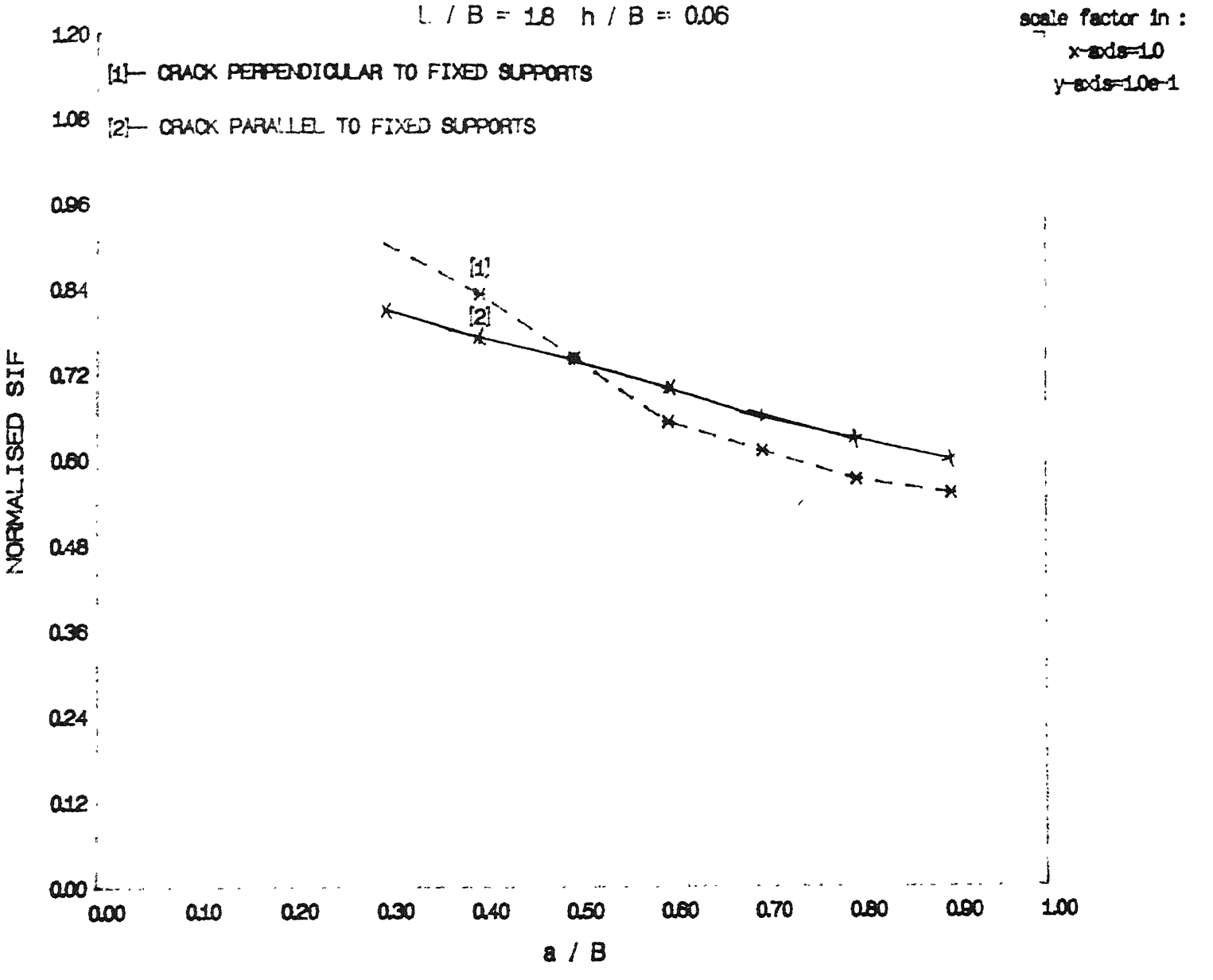

Fig. 3.16 Effect of crack orientation on normalised SIF (Simply Supported ends)

influenced by the moment reactions at the fixed supports. Whereas the limiting h/B value, upto which the thin plate theory is valid is slightly more than case (A), on the other hand the L/B value beyond which effect of boundary conditions vanishes is the same.

(C) Orientation effect

It is seen from Fig. 3.12 that for a thin square plate (L/B = 1.0, h/B = .025) a crack perpendicular to the fixed supports has the larger normalised SIF than crack parallel to supports. Thus a perpendicular crack is more dangerous than a parallel crack. As the thickness is increased (h/B = 0.20) the difference becomes smaller (Fig. 3.13). When the length is increased the difference becomes even smaller (Fig. 3.14). Fig. 3.15 shows that for a long and thick plate (L/B = 1.5, h/B = 0.20) the curves nearly coincide. Thus when both 'L' and 'h' increase the normalised SIF becomes independent of the orientation. However for moderately thick plates the curves can cross each other when L/B is sufficiently large. This means that critical orientation now depends on a/B ratio (Fig. 3.16). It can be observed that his critical a/B ratio is around 0.45.

3.2.2 Case with free ends

(A) Crack parallel to fixed supports

It can be seen from Fig. 3.17 and 3.18 that the trend of variation of normalised SIF with respect to the crack length, plate thickness and plate length are similar to the earlier case (i.e. when the edges are simply supported). When the other edges are free, the entire transverse load is supported by the fixed supports. This leads to substantially higher values of support

reactions which in turn raise the levels of bending moment in the neighbourhood of the crack to great extent. Because of this the normalised SIF values are significantly higher when the other edges are free. It is also observed that limiting values of L/B and h/B are also considerably higher (L/B = 2.2, h/B = .025).

(B) Crack perpendicular to fixed supports

When the other two edges are free, the case of perpendicular crack is very interesting. Here the trends of variation of the normalised SIF with respect to a/B, h/B and L/B are completely different than all the three previous cases. As far as variation with a/B is concerned, unlike in other cases it is quite sharp in the lower range of a/B. Further the change in the normalised SIF with respect to either the plate thickness or the plate length is very insignificant. It has been observed earlier that as the boundary conditions change from simply supported to free the value of normalised SIF increases. It is also seen that value of normalised SIF increases as the crack orientation changes from parallel to perpendicular. In this case, due to the cumulative effect of above two factors the value of normalised SIF is very high.

(C) Orientation

It has been observed in section 3.2.2(B) that for a perpendicular crack, the length and thickness have insignificant effect on the value of normalised SIF. So with increase in 'L' or 'h' only the curve with parallel crack orientation shifts (Fig. 3.21 - 3.24). As the variation with a/B is different, the curves cannot coincide completely. It can be seen that for lower values

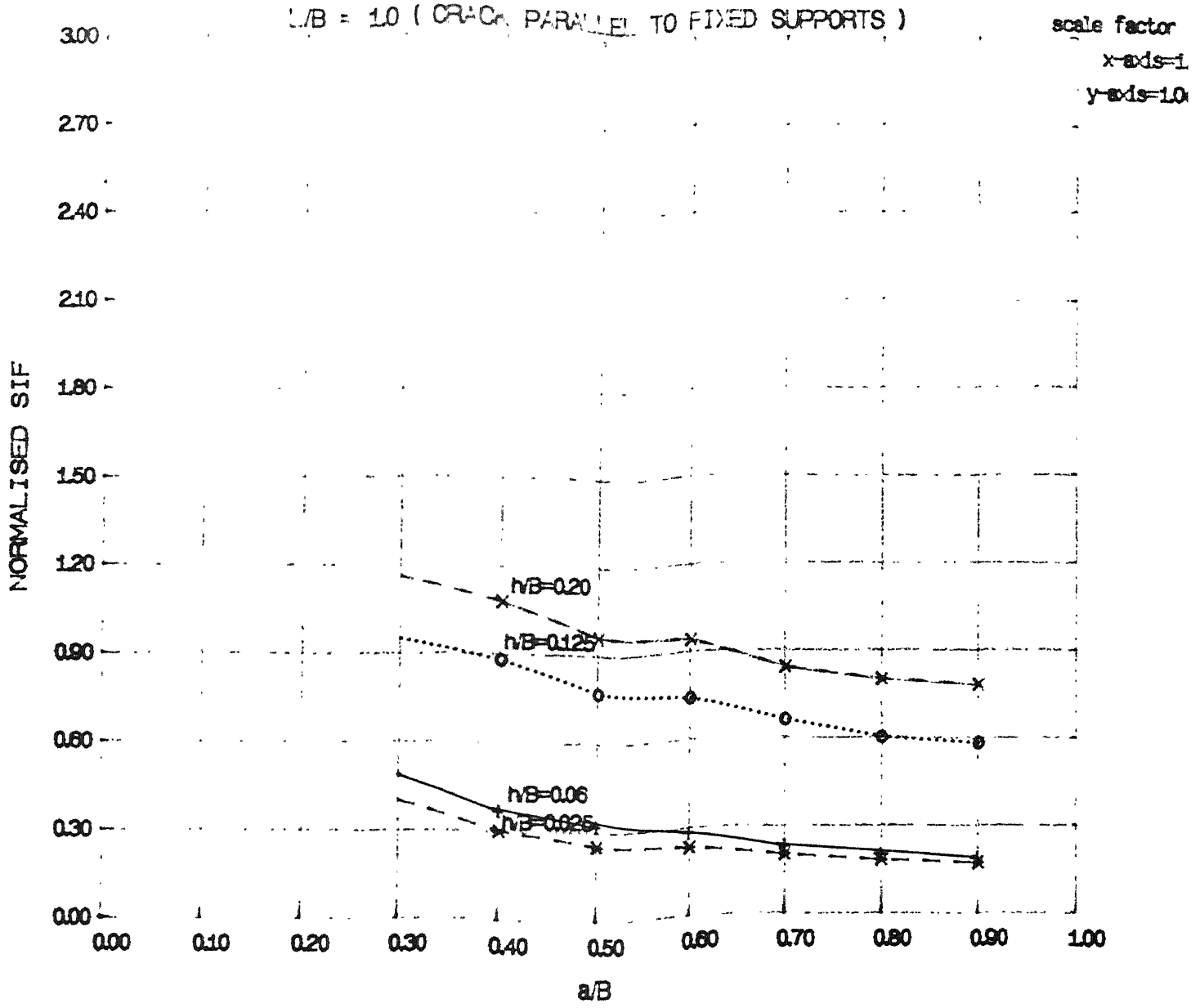

Fig. 3.17 Effect of h/B ratio on normalised SIF (free ends)

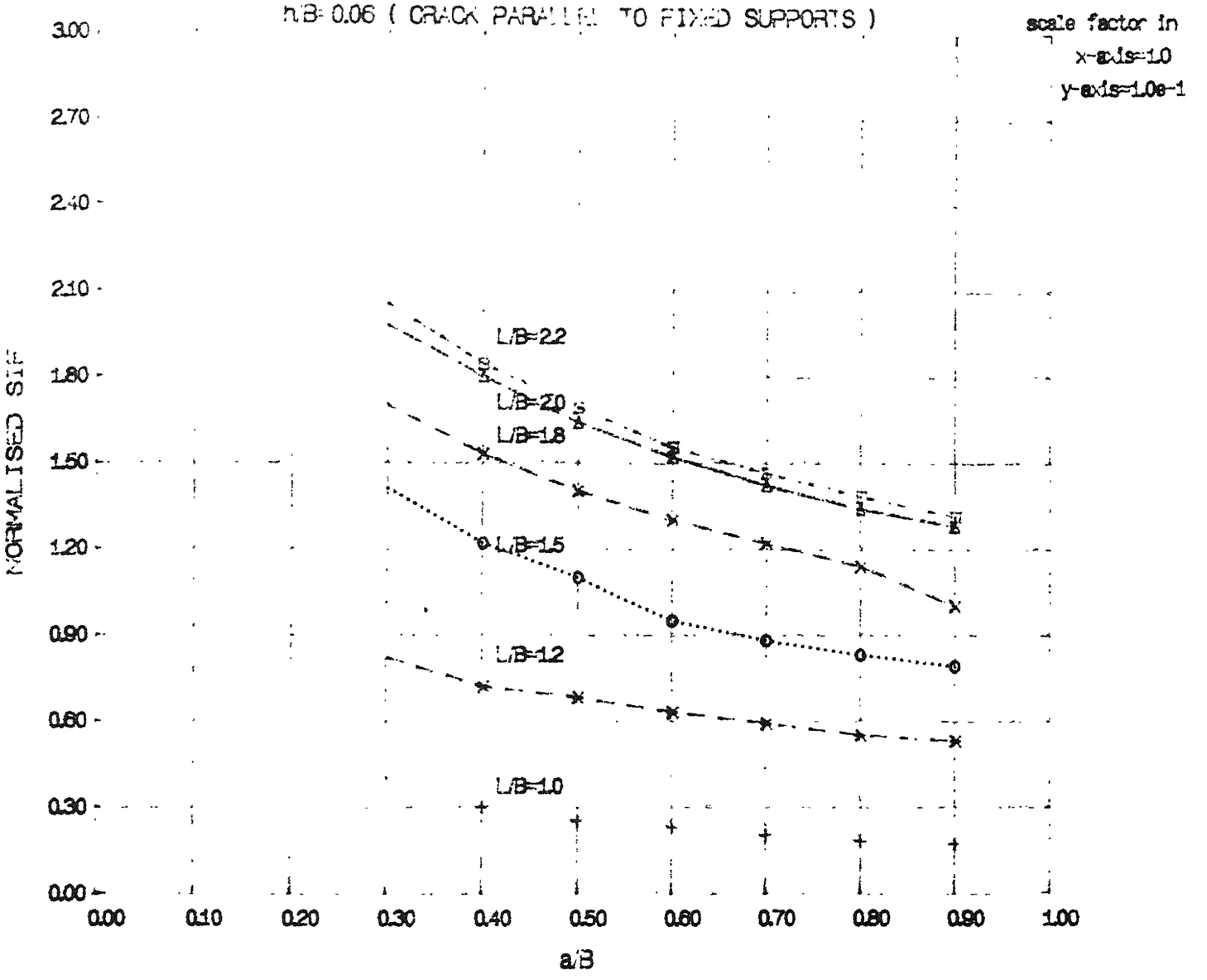

Fig. 3.18 Effect of L/B ratio on normalised SIF (free ends)

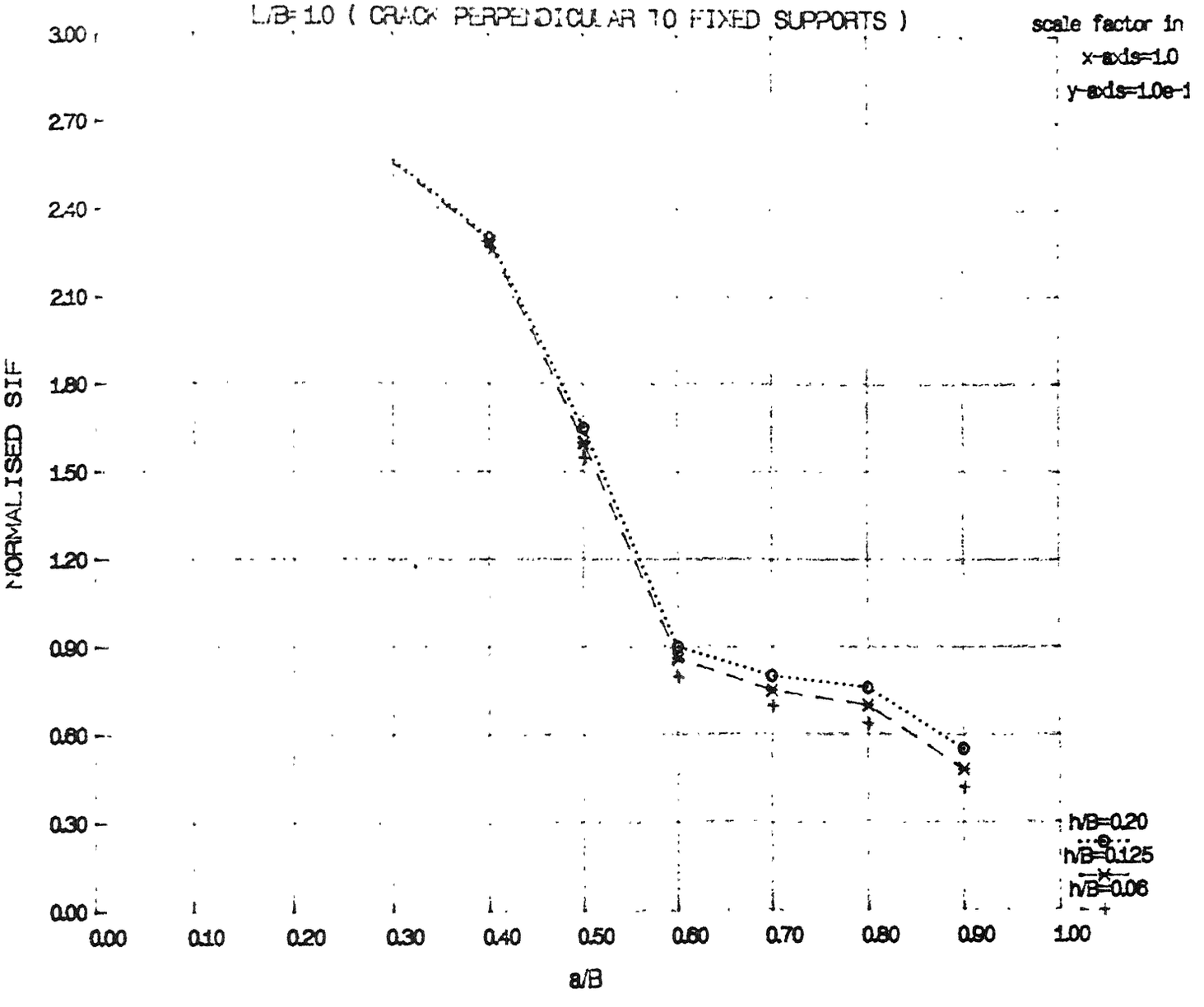

Fig. 3.19 Effect of h/B ratio on normalised SIF (free ends)

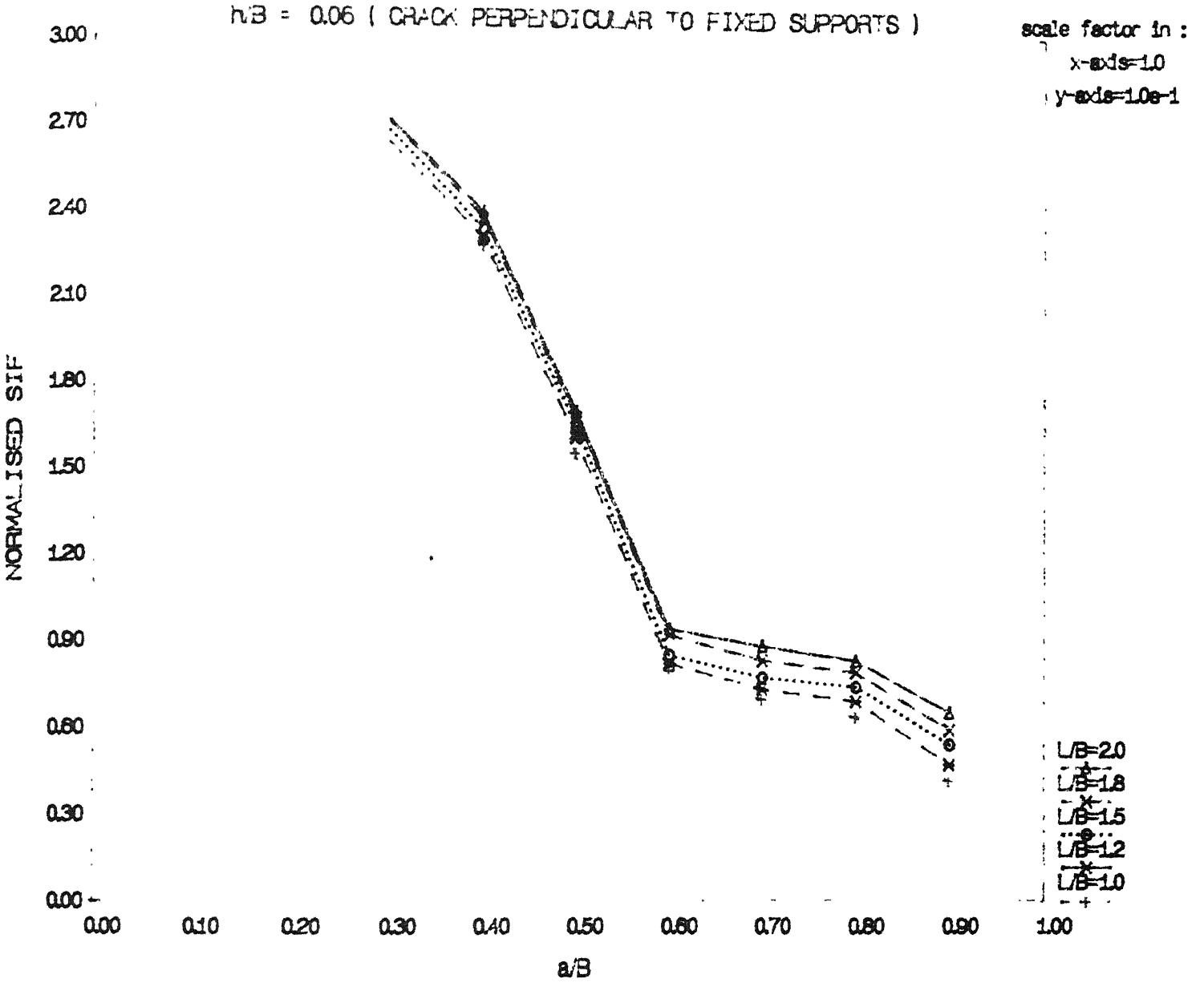

Fig. 3.20 Effect of L/B ratio on normalised SIF (free ends)

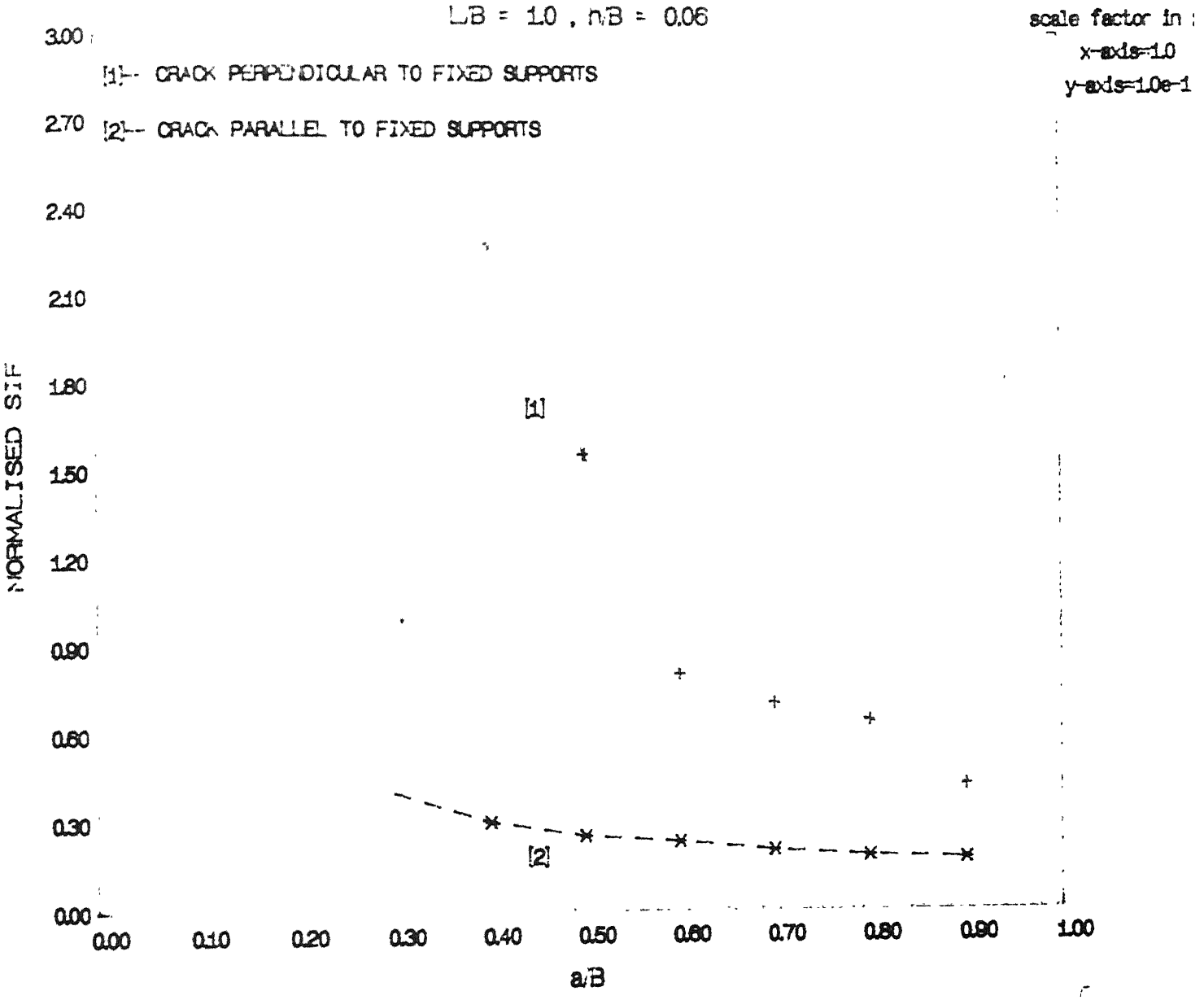

Fig. 3.21 Effect of crack orientation on normalised SIF (free ends)

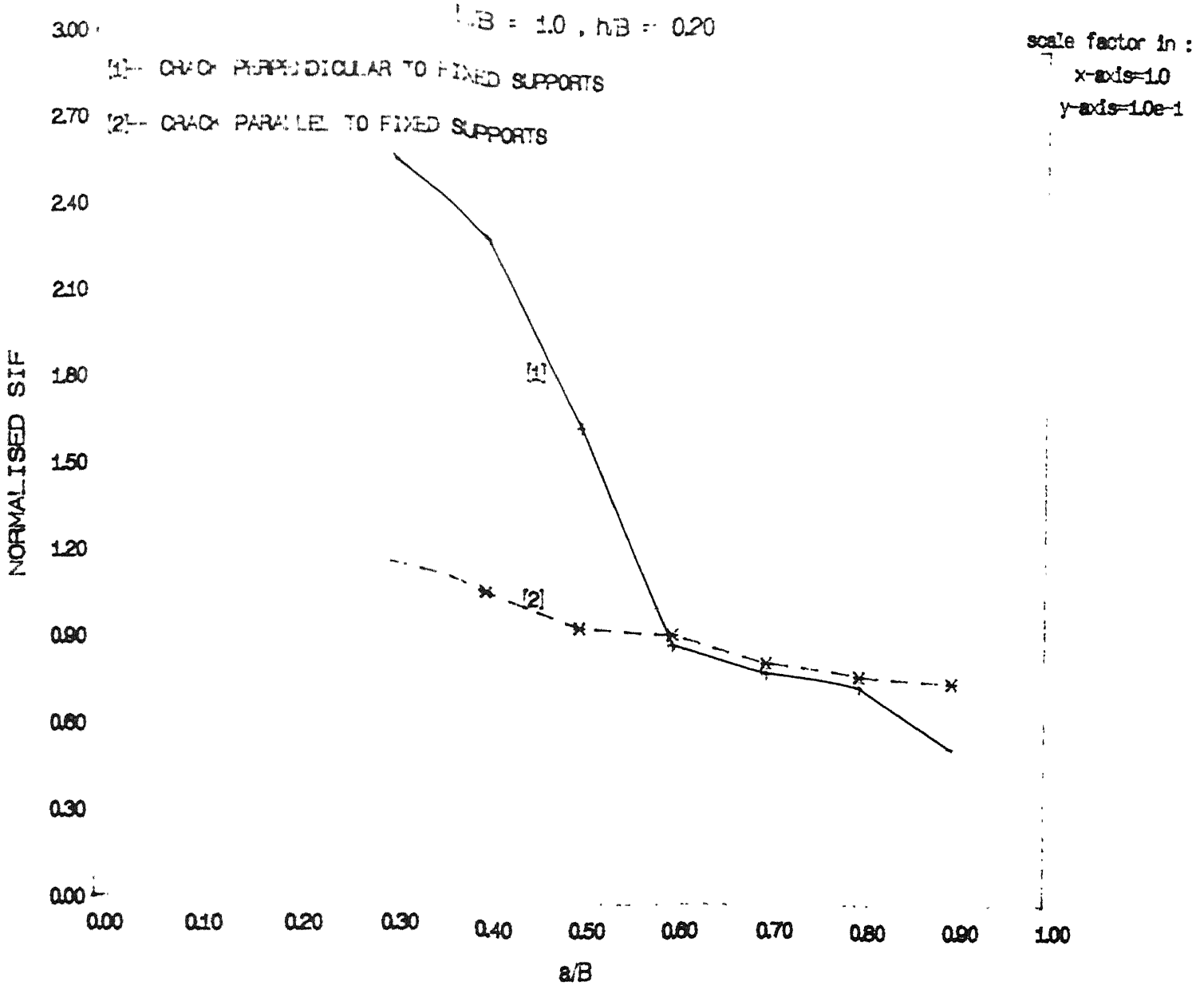

Fig. 3.22 Effect of crack orientation on normalised SIF (free ends)

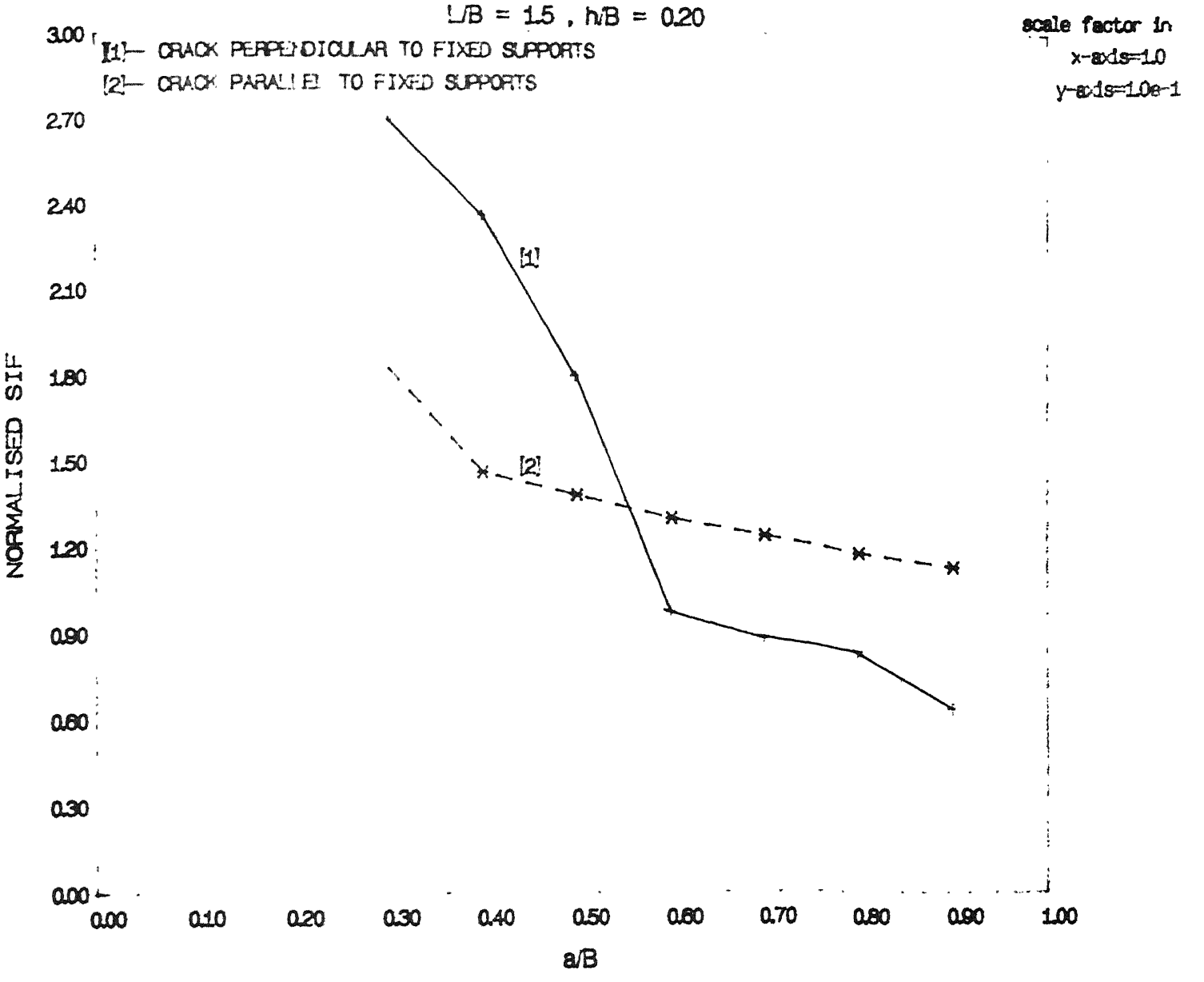

Fig. 3.24 Effect of crack orientation on normalised SIF (free ends)

of a/B the orientation effect is observed while for higher a/B ratios the effect vanishes.

3.3 Conclusions

In the present work a part of submarine hull subjected to a transverse load has been idealised as a plate. It has been assumed that the two ends of the plate mounted on circumferential stiffening rings have fixed boundary conditions and the distance between them remains constant. Effect of plate thickness, plate length, crack orientation and boundary conditions on normalised SIF has been studied. The following conclusions can be drawn from this work.

(1) It is well-known that as the plate thickness (h) is decreased beyond a certain value, the thin plate theory becomes valid and as a result the normalised SIF becomes independent of it. In our case the limiting value of h/B is between 0.02 to .025, the lower value being applicable to the case of parallel crack and simply supported boundary conditions.

(2) It is observed that normalised SIF increases with L/B ratio except for the case of perpendicular crack with free supports. It is further observed that for a simply supported case the limiting value of L/B ratio after which the effect of boundary conditions vanishes is 2.0. For the free case with parallel crack the limiting value is 2.2.

(3) It is observed that for a simply supported case for L/B = 1.5 and h/B = 0.20, SIF becomes independent of orientation, while for a free case such a behaviour is not observed.

(4) It is seen that value of normalised SIF increases as the boundary conditions change from simply supported to free, and as the orientation changes from parallel to perpendicular. It can be said that a perpendicular crack with free ends is the most dangerous.

3.4 Suggestions for future work

The finite element model can be improved by using a degenerate solid element with five degrees per node, so that the membrane effect can be modelled accurately. The analysis can be extended to include elasto-plastic dynamic behaviour. The present idealisation of submarine hull as a plate can be modified to a cylindrical ring (shell) analysis to avoid uncertainty of boundary conditions.

References

1. M.L. Williams, The bending stress distribution at the base of a stationary crack, J. Appl. Mech. Trans. ASME 28, 78-82 (1961).

2. G.C. Sih and J.R. Rice, The bending of plates of dissimilar materials with cracks, J. Appl. Mech, Trans. ASME 31, 477 (1964).

3. G.C. Sih and J.R. Rice, Author's closure of discussion of "The bending of plates of dissimilar materials with cracks", J. Appl. Mech., Trans. ASME 32, 464 (1965).

4. Mindlin R.D., Influence of rotatory inertia and shear on flexural motions of isotropic elastic plates. J. of Appl. Mech. 18, 31-38 (1951).

5. E. Reissner, The effect of transverse shear deformation on the bending of elastic plates, J. Appl. Mech., Trans. 12, A-69 (1945).

6. W. Yang and L.B. Freund, Transverse shear effects for through-cracks in an elastic plate, Int. J. Solids Structures 21, 977-994 (1985).

7. R.J. Hartancraft and G.C. Sih, Effect of plate thickness on the bending stress distribution around through cracks, J. Math. Phys. 47, 276-291 (1968).

8. M.V.V. Murthy, K.N. Raju and S. Viswanath, On the bending stress distribution at the tip of a stationary crack from Reissner's theory, Int. J. Fracture 17, 537-552(1981).

9. N.N. Wahaba, On the use of singular displacement finite elements for cracked plates in bending, Int. J. Fracture 27, 3-30(1965).

10. S. Viswanath, M.V.V. Murthy, A.V. Krishnamurthy and K.P. Rao, A special crack tip element for bending of plates with through cracks from a sixth order plate theory, Engg. Fracture Mech., 32, 91-109 (1989).

11. G. Yagawa and T. Nishioka, Finite element analysis of stress intensity factors for plane extension and plate bending problems, Intr. J. Numer. Meth. Engg. 14, 727-740 (1979).

12. Y. Yamada, Y. Ezawa and I. Nishiguichi, Reconsiderations on singularity or crack tip elements, Intr. J. Numer. Meth. Engg., 14, 1525-1544 (1979).

13. R.S. Barosum, A degenerate solid element for linear fracture analysis of plate bending and general shells, Intr. J. Numer. Meth. Engg., 10, 515-564 (1976).

14. R.S. Barosum, triangular quarter point elements as elastic and perfectly plastic crack tip element, Int. J. Numer. Meth. Engg., 11, 85-98 (1977).

15. H. Sosa and J.W. Eischen, Computation of stress intensity factors for plate bending via a path independent integral, Engg. Fracture mech., 25 (No. 4), 451-462 (1986).

16. H. Sosa and G. Herrmann, on invariant integrals in the analysis of cracked plates, Intr. J. of Fracture, 40, 111-126 (1989).

17. G.C. Sih, Strain energy density factor applied to mixed mode crack problems, Inter, J. of Fracture, 10, 305-321 (1974).

18. G.C. Sih, A three dimensional strain energy density factor theory of crack propogation, three dimensional crack problems, Mechanics of Fracture II, edited by G.C. Sih, Noordhoff Publishing, 15-33 (1975).

19. E. Hinton and D.R.J. Owen, Finite Element Softeare for plates and shells, Pineridge Press Swansea, U.K., 157-233.